AALTO YLIOPISTO
FACULTY OF PHYSICS AND APPLIED MATHEMATICS
SYSTEMS ANALYSIS LABORATORY

Emission estimation of marine traffic using vessel characteristics and AIS-data

Master's Thesis

Lasse Johansson

9/19/2011

Supervisor: Prof. Harri Ehtamo

Instructors: Ph.D. Jukka-Pekka Jalkanen, prof. Jaakko Kukkonen

AALTO UNIVERSITY 11000, 00076 Aalto http://www.aalto.fi	ABSTRACT OF THE MASTER'S THESIS

AUTHOR: Lasse Johansson

TITLE: Emission estimation of marine traffic using vessel characteristics and AIS-data

TITLE IN FINNISH:
Laivapäästöjen mallinnus AIS-dataan ja aluskohtaisiin tietoihin perustuen

FACULTY: Faculty of information and natural sciences

DEGREE PROGRAMME: The department of physics and applied mathematics

MAJOR: Systems analysis (F3008)	MINOR Industrial management and engineering

Supervisor: Prof. Harri Ehtamo
Instructors: Ph.D. Jukka-Pekka Jalkanen, Prof. Jaakko Kukkonen

Based on the STEAM model at the Finnish Meteorological Institute, an extended method is presented for the evaluation of the exhaust emissions of marine traffic. The model uses detailed technical data of each individual vessel and also messages provided by the Automatic Identification System (AIS), which enable the positioning of ship emissions with a high spatial resolution (typically a few meters). The presented Ship Traffic Emissions Assessment Model (STEAM2) allows for the influences of accurate travel routes and ship speed, engine load, fuel sulfur content, multiengine setups, abatement methods and waves.

The previously developed model was applicable for evaluating the emissions of NO_x, SO_x and CO_2. The extended version addresses also the mass-based emissions of particulate matter (PM) and carbon monoxide (CO). Compared to the previous version, a more detailed power and fuel consumption estimation process is introduced and the model's performance is evaluated against available experimental data on engine power, fuel consumption and the composition-resolved emissions of PM.

Several ways for improving the model further are also presented. This includes the addition of kinetic energy of the individual ships, the addition of sea currents and a sub program to process AIS data before it is used for modeling.

Finally, the model is used for estimating emissions and shipping statistics from marine traffic in the Baltic Sea during 2006 and 2009 and based on these results, the most contributing flag states and ship types are identified. The geographical shifts in the marine traffic are visualized with a difference map and the effect of a sulfur reducing legislation is quantified.

Date: 19.9.2011	Language: English	Pages: 81

Keywords: emission estimation, STEAM, AIS, marine traffic, particle matter emissions

AALTO YLIOPISTO 11000, 00076 Aalto http://www.aalto.fi	DIPLOMITYÖN TIIVISTELMÄ

TEKIJÄ: Lasse Johansson

TYÖN NIMI: Laivapäästöjen mallinnus AIS-dataan ja aluskohtaisiin tietoihin perustuen

TIEDEKUNTA: informaatio- ja luonnontieteiden tiedekunta

OPINTO-OHJELMA: Teknillinen fysiikka ja matematiikka

PÄÄAINE: Systeemianalyysi (F3008)	SIVUAINE: Teollisuustalous

Valvoja: Prof. Harri Ehtamo
Ohjaajat: Ph.D. Jukka-Pekka Jalkanen, Prof. Jaakko Kukkonen

Tässä työssä esitellään laajennettu ja paranneltu versio laivojen pakokaasupäästöjen mallintamiseen perustuen Ilmatieteen laitoksen laivapäästömalliin (STEAM). Suurille laivoille pakollisen automaattisen viestijärjestelmän (AIS) ja kattavan laivatietokannan avulla laivojen paikka- ja nopeustiedoista voidaan laivoille estimoida päämoottorien kuormitusasteet ja polttoaineen kulutus. Ottaen huomioon mm. käytetyn polttoaineen laadun, mahdolliset asennetut päästövähennyslaitteistot ja laivaa ympäröivän aallokon, voidaan mallilla estimoida laivojen pakokaasupäästöjen maantieteellistä jakautumista ja kokonaispäästömääriä Itämerellä.

Mallin aikaisemmin julkaistu versio sisälsi hiilidioksidipäästöjen lisäksi ihmisille haitallisten rikin ja typen oksidien mallintamisen. Työssä esiteltävä laajennettu päästömalli estimoi näiden lisäksi myös laivojen partikkeli- ja hiilimonoksidipäästöt. Lisäksi, laajennetussa mallissa käytetään paranneltua tehon ja polttoaineen kulutuksen estimointitapaa, joka ottaa huomioon laivan fyysiset mitat. Laajennetun mallin ennustustarkkuutta verrataan kokeellisesti mitattuja teholukemia vastaan. Tämän lisäksi laivayhtiöiden antamia vuosittaisia polttoaineen kulutusarvoja verrataan mallin tuottamiin ennusteisiin.

Mallin tuottamia Itämeren laivapäästötuloksia vuosille 2006 - 2009 esitellään työssä yksityiskohtaisesti. Vuosina 2008 ja 2009 Euroopan taloutta ravisutelleen laskusuhdanteen vaikutukset laivaliikenteeseen arvioidaan sekä Itämeren maat järjestetään niiden laivastojen päästömäärien mukaiseen järjestykseen. Lisäksi, laivaliikenteen maantieteellisiä muutoksia tutkitulla aikavälillä havainnollistetaan sekä vuonna 2006 voimaan tulleen merkittävän rikkidirektiivin vaikutuksia esitellään.

Työssä esitetään lukuisia tapoja joilla laajennettua mallia voidaan jatkokehittää, kuten merkittävien merivirtojen sisällyttämisen malliin, AIS-datan esikäsittelyn sekä laivojen kiihdytysvaiheen tarkemman mallinnuksen.

Päivämäärä: 19.9.2011	Kieli: englanti	Sivumäärä: 81

Avainsanat: emission estimation, STEAM, AIS, marine traffic, particle matter emissions

TABLE OF CONTENTS

Abbreviations

OC	Organic carbon
EC	Elemental carbon
NO_X	Nitrogen oxides
SO_X	Sulphur oxides
CO	Carbon monoxide
SO_4	Sulphate
CO_2	Carbon dioxide
PM	Particle matter, defined as the sum of OC, EC, Ash, SO_4 and its associated water
STEAM	Ship Traffic Emission Assessment Model
RPM	Revolutions per minute
AIS	Automatic identification system
Helcom	Helsinki Commission, Baltic environmental protection commission
IMO	International Marine Organization
IMO GHG2	IMO Greenhouse gas study, published in 2009
SECA	Sulfur emission control area
TEU	Twenty-foot equivalent unit, a measure used for capacity in container transportation
SFOC	Specific fuel-oil Consumption
CAT	Caterpillar, engine manufacturer

RoPax	Roll-on, Roll-off passenger ship
RoRo	Roll-on, Roll-off vehicle carrier ship
MMSI	Maritime mobile service identity, a series of nine digits which are sent in digital form over a radio
GT	Gross tonnage of a ship
DWT	Deadweight of a ship
LOA	Length overall in meters
LBP	Length between perpendiculars in meters
LNG	Liquid natural gas

Symbols and notations

F_{water}	Resistance force resulting from moving in water (turbulence, waves, displacement of water)
F_P	Propelling force of the ship
F_{Env}	Resistance force component which is in parallel to the speed vector. F_{Env} is caused by the surrounding environment (wind, air and ambient waves)
F_{Fr}	Resistance force resulting from friction induced to the wet surface of the ship
η_{qpc}	Quasi-propulsive constant, a ship specific efficiency ratio of the ship's propeller which is the ratio of F_P and generated shaft force of the engine

$v(t) = \|\mathbf{v}\|$	Speed of the ship
$a(t)$	Acceleration
$a_{eff}(t)$	Effective acceleration of the ship which is caused by engine use
$P(t)$	Instantaneous power requirement in kW
P_S	Service power rating of a ship
RPM_{Pr}	Number of revolution per minute of a propeller
d	Propeller diameter
C_B	Block coefficient
$\boldsymbol{F_n}(t)$	Froude number
EL	Engine load
$SFOC_{base}$	Base value for the specific fuel-oil consumption of an engine
$SFOC_{Relative}$	Relative value of SFOC compared against the minimum value
m	Mass of a ship, defined as the sum of gross tonnage and deadweight
m_{SO_X}	Mass of the SO_X particle in grams
$\frac{dN_{SO_X}}{dt}$	Conversion rate of the SO_X particle in combustion process, particles formed per time interval
EF_{CO}	Emission factor measured in g/kWh for CO
CO_{base}	Base value for carbon monoxide emission factor

EF_{PM}	Emission factor measured in g/kWh for total PM emissions
EF'_{PM}	Revised emission factor for PM emissions
ABC	Acceleration based component of CO emission factor
$\mathbf{v}_C$	Velocity vector of a current
v_{CP}	Speed component of $\mathbf{v}_C$ which is in parallel with the ship's velocity
t	Time, combustion time
C_{str}	Stroke type dependent coefficient for determining combustion process time
r_{HV}	Ratio of heat values of LNG and diesel fuel oil
m_{CO2LNG}	The mass of CO_2 produced by combusting one gram of LNG fuel
$m_{CO2Diesel}$	The mass of CO_2 produced by combusting one gram of diesel fuel

Acknowledgements

I would like to thank the Finnish Meteorological Institute for giving me this opportunity to contribute to their novel way of modeling ship emissions. I am grateful for the open minded and helpful atmosphere of the co-workers (especially Jukka-Pekka Jalkanen, the original creator of STEAM model) which made possible to edit the model source code quite freely to gain better insight of the model itself. I would also like to thank Jaakko Kukkonen for his editorial contribution and for the guidance which has made me a better writer in scientific literature. Furthermore, it would not have been possible to produce such an extensive representation of the model along with its validation data by the author himself and it should be noted that especially chapters 3 and 5 contain a significant contribution from the instructors of this thesis.

1. Introduction

Emissions from shipping have a significant impact on ambient air quality in densely populated coastal areas. Indeed, emission smog rising from the busiest ship routes in the world are clearly visible from space. The marine exhaust emissions may substantially contribute to detrimental impacts on human health; a study made by Corbett et al. estimates that the annual premature mortality caused by shipping will be approximately 87 000 premature deaths annually in 2012 if shipping emissions are not further regulated (Corbett et al., 2009). A more recent study, however, suggests that the contribution of shipping might be even greater - Particle matter (PM) emissions alone are estimated to be responsible for the loss of 1.8 million years of life lost including 1.3 million years of life lost due to mortality in the studied six countries of Belgium, Finland, France, Germany, Italy and the Netherlands, making PM the most significant environmental factor affecting public health (Hänninen et al. 2011). The contribution of shipping sector to the amount of PM in coastal urban areas such as Helsinki, Rotterdam and Los Angeles have been estimated to be significant, ranging from 13% up to 42% depending on the geographical area of measurements (Starcrest, 2008).

Besides particle emissions, marine shipping causes significant carbon monoxide (CO_2), nitrogen and sulfate oxide emissions (NO_X, SO_X), which in turn affect the public health and increase the amount of acid rain. Moreover, sulfur and nitrogen oxides in marine exhaust gas have been reported to affect cloud formation process in the lower atmosphere due to the so-called indirect aerosol effect – the particles are able to act as cloud condensation nuclei (Schreier et al., 2006).

The yearly monetary cost of the health problems that are associated with marine traffic is a subject of debate in recent literature. Depending on the contribution of marine traffic to the total PM emissions, the yearly monetary cost is likely to be in several billion of euros in Europe alone. Because of the high costs, stringent limits for the sulphur content of marine fuels and for NO_X emissions are being introduced, which are expected to reduce the emissions from ships. As a result, PM emissions would be simultaneously reduced, as a major part of PM emissions is in the form of sulphate. However, sulphur content reductions will not eradicate PM emissions completely (Winnes and Fridell, 2010; Fridell et al., 2008; Cooper, 2006; Cooper, 2003; Kasper et al., 2007; Buhaug et al., 2009), even if the global fleet would switch to low sulphur fuel.

The emissions of *PM* can also be reduced by using after-treatment techniques, which will remove a significant part of the *PM* emissions (Corbett et al., 2010; European Commission Directorate General Environment, 2005) Scrubbing systems from engine manufacturers have been commonly applied to diesel power plants on land, but their commercial installations to ships have been scarce. This is expected to change, after the implementation of the stringent sulphur limits included in the revised Marpol Annex VI of the IMO (International Maritime Organization, 1998).

Policy makers cannot effectively reduce health problems caused by marine traffic without sufficient and timely information about the total amounts and geographical distribution of the emissions. Therefore emissions are estimated with several different models that produces information about where, how much and by whom emissions are being released into the atmosphere. Currently available global ship emission inventories are mostly based on top to down (i.e., top-down) –approaches in which emission estimates are made using fuel statistics and known ship routes without considering single vessel characteristics. However, the statistics concerning the sales of marine fuels are difficult to disaggregate to the amounts of fuel burned regionally or locally. The approaches based on fleet activities, called as bottom-up methods, have therefore recently gained popularity; new ship emission inventories have been generated especially for arctic regions (Paxian et al., 2010; Corbett et al., 2010). Various regional ship emission inventories have been introduced (Matthias et al., 2010; De Meyer et al., 2008) and the previously significant uncertainties in the estimated emissions of global ship traffic have been evaluated to have decreased during the last half decade (Paxian et al., 2010; Lack et al., 2008). Information is currently scarce especially regarding the geographical distribution and chemical composition of *PM* emissions arising from ship traffic, and the chemical composition details have not commonly been introduced to global bottom-up inventories of ship emissions.

In 2009, presented at the Finnish Meteorological Institute, a bottom-up method for the evaluation of the exhaust emissions of marine traffic was introduced. The model was based on the messages provided by the Automatic Identification System (AIS), which enable the identification and location determination of ships (Jalkanen et al., 2009). The use of the AIS data facilitates the positioning of ship emissions with a high spatial resolution, which is limited only by the inaccuracies of the Global Positioning System (typically a few meters). Using the AIS data for emission estimation almost totally

removes the inaccuracies that are caused by the uncertainties of evaluating the times of ships spent at sea and at berth. The instantaneous speeds of the vessels are also known from the AIS data, the use of which substantially reduces the uncertainties in analyzing the operational states of the ship engines. The methodologies for evaluating the power and fuel consumption, however, were fairly simple in the introduced model version, and the assumptions of the model were observed to provide biased estimates especially for auxiliary engines. In this paper, an extended version of the emission estimation model is presented.

The main objectives of this thesis are *(i) to introduce and evaluate the extended model and its new features for marine emission modeling, (ii) to present ways to improve the extended model even further and (iii) to present emission estimations and shipping traffic analysis produced by the model about marine traffic in the Baltic Sea.* The modelled emission types and their effect on human health are briefly discussed in Chapter 2. In Chapter 3 the extended model with its principles and mathematical structure, including the model's recent adjustments such as more sophisticated scheme for the resistance evaluation and a load balancing of the engine, are introduced.

Chapter 4 includes the discussion of the challenges that have been encountered after extensive use of the extended model and also, some solutions for these problems and new modifications to the model are presented. Most of the changes for the model that are suggested in this chapter however, are currently being implemented and thus are not affecting emission estimates presented in this thesis.

The main results of this thesis are presented in Chapter 5 and 6, followed by discussion and conclusions of the results in Chapter 7. In chapter 5, the model's capability to predict instantaneous power requirements and fuel consumption is evaluated against available experimental data and emission factors provided by the model are compared to the available measurements presented in recent literature. In Chapter 6 the total emission estimates for the Baltic Sea shipping between January 2006 and December 2009 are presented. As a byproduct to the emission estimate outputs, the statistical data produced by the model is put into use and the flag states and ship types, that are making the biggest contribution, are identified. Also, geographical shifts in marine traffic during the recent years are identified and the effect of the late recession in Europe is studied.

2. Exhaust emissions of diesel engines and their effect on human health

In the diesel engine combustion process, high pressured fine droplets of diesel fuel are mixed with air and the mixture spontaneously combusts after being heavily pressurized.. For a typical 2-stroke marine diesel engine, which uses 170 grams of fuel per produced kWh, 7.8 kg of air is used as the combustion process requires large amount of oxygen (21% in volume of air). In the combustion process, volatile carbon compounds react with oxygen forming carbon dioxide CO_2 and water, simultaneously releasing significant amount of heat. The exhaust gas (170g of fuel per kWh) contains approximately 0.5 kg of CO_2, 0.2kg of vaporized water and also 1.1kg of excess oxygen (Kuiken, 2008). The increase in heat in the combustion chamber causes thermodynamic expansion and piston movement, which is converted to mechanical work for the rotating crankshaft. The movement of the pistons causes friction and thus a constant supply of lube oil is needed. For a typical engine, the need of lube is a couple of grams per kWh but may contain heavy and alkaline metals, which are released in the exhaust gas as the lube oil gets perfectly combusted in the process as well.

Besides CO_2 and the small amount of heavy metals, significant amount of harmful material is released to the atmosphere in the exhaust gas that causes direct and indirect detrimental effects to human health and to the environment, such as NO_x, SO_x, CO, and PM. These pollutants and their effects on human health and to the environment are briefly discussed here. The pollutants react in atmosphere with various complex chemical interactions. Some chemical interactions start immediately in the early plume phase making the measurement of emissions directly from exhaust plumes challenging. These chemical reactions and their effect thereafter, however, are beyond the scope of this thesis.

2.1.1 Carbon monoxide (CO) and carbon dioxide (CO_2)

$CO_2$is the main product resulting from the combustion of fossile fuel and is not harmful for human health but is well known for its effect on increasing the radiative forcing on Earth's surface $[W/m^2]$. In other words, CO_2 enforces the phenomenon called the greenhouse effect.

Carbon monoxide is a colorless and odorless gas which is a product of incomplete combustion of organic matter due to insufficient oxygen supply to enable complete oxidation to carbon dioxide. Mild exposures to CO may cause headaches, vertigo, and flu-like effects, but larger exposures (at 100ppm or greater) can lead to significant toxicity of the central nervous system and heart, and even death. (Prockop L, Chichkova, R., 2007).

2.1.2 Nitrogen oxides (NO_x)

Air is mostly (78%) nitrogen and thus large amount of nitrogen gets mixed in the combustion process. Nitrogen is an inert gas that doesn't under normal circumstances combust with other substances. In diesel engine combustion process, however, the temperature rises up to $2000°K$, which is more than sufficient to enable nitrogen combustion.

Nitrogen oxides are precursor components for a photochemical reaction in which ozone is formed in the lower atmosphere (Brunekreef et al., 2002). Nitrogen dioxide is also a catalyst compound for the formation H_2SO_4 and thus for acid rain. Exposure to ozone can lead to a variety of respiratory health effects, such as coughing, throat irritation and reduced lung function. In addition, it can worsen bronchitis, emphysema, and asthma. (Hänninen et al., 2011)

2.1.3 Sulfur oxides (SO_x)

Currently in 2011 inside the sulfur emission control area (SECA) which contains the Baltic Sea, marine diesel-oil contains sulfur compounds up to 1% of mass and before May 2006 the maximum allowed sulfur level was as much as 2.7%. The combustion process generates significant amount of sulfur oxides, especially SO_2 and SO_3. When released in to the atmosphere, SO_X is further oxidized, usually in the presence of a catalyst such as NO_2, forming H_2SO_4 and thus is causing acid rain. Emitted SO_2 particles with its direct and indirect effects are making the largest non-greenhouse contribution of shipping to global climate forcing. (Petzold, 2010). The direct aerosol forcing of sulfate particles from shipping ranges between $-47 * 10^{-3}\, Wm^{-2}$ and $-12 * 10^{-3}\, Wm^{-2}$ and thus balances the positive radiative forcing effect of CO_2.

The range of the released SO_X particles is limited to a few hundred kilometers depending on weather and wind conditions. Because of this, most of the SO_X emissions

at open sea end up being neutralized by sea water and are not believed to pose a direct threat to human health.

2.1.4 Particulate matter (PM)

Unlike other emissions, which are chemically defined, particulate matter (PM) is defined in international standards (ISO 8178) as the mass that is collected on a filter under specified conditions. The chemical composition as well as the size distribution, however, varies in literature. In this paper, PM (diameter $\leq 2.5\mu m$) from marine emissions is defined to include ash particles, organic (OC) and elementary carbon (EC) and sulphate (SO_4) and its associated water molecules. Fuel sulphur content has been observed to affect significantly to the amount of PM emissions because all of the sulphate and its associated water molecules originate from the sulphur content of the fuel.

PM is the most thoroughly internationally reviewed environmental pollutant during the last decade. The health implications of the particulate matter components have been extensively studied and convincing epidemiological evidence associates PM mass concentrations with the health impacts (Hänninen et al. 2011). Exposure to PM has been associated with both respiratory and cardiovascular effects and total mortality. PM emissions have been estimated to cause a loss of 1.8 million years of life lost annually, including 1.3 million years of life lost due to mortality in the studied six countries of Belgium, Finland, France, Germany, Italy and the Netherlands (Hänninen et al. 2011). Overall 67 % of the estimated environmental burden of disease in the study of Hänninen et al. was explained by exposure to PM making it the most significant environmental factor affecting public health.

2.2 Abatement methods and reduction potential of emissions

Although it is possible to remove CO_2 from exhaust gases by chemical conversion, this is not considered feasible. A number of options for improvements in efficiency and thus for reducing fuel consumption and CO_2 however, are readily available. The potential for fuel savings can be very significant (20% - 75%), but at the same time the costs, lack of incentives and other barriers may prevent many of the efficiency improvements from being adopted (Buhaug, 2009).

Significant reductions of SO_X emissions can be achieved through limitations on the sulfur content of fuel. Other possibility to reduce the level of SO_2 is the installation of an exhaust-gas scrubbing system. Two main principles exist for the scrubbing system: open-loop seawater scrubbers and closed-loop scrubbers. Both scrubber concepts may also remove PM and limited amounts of NO_X (Buhaug, 2009). Emissions that are removed from the exhaust are carried in the wash water and released to the sea. After being released, sulphur oxides react with the seawater to form stable compounds that are normally abundant in seawater and are not believed to pose any danger to the environment and human health.

PM emissions and especially sulphate particles can be reduced by scrubbing with seawater. Claims for the potential reduction of PM emission levels range from 90% to 20% depending on the particle size distribution as the smaller emission particles are very difficult to extract from the exhaust gas. Emissions of PM can be further reduced by optimizing combustion process, for example by achieving better oxidization and minimizing of the lube oil consumption as well as the additives in lube oil itself. The burning of fuel–water emulsions can also reduce emissions of PM to a certain extent, but may cause reductions to the efficiency of the engine.

Emissions of NO_X from diesel engines can be reduced by a number of measures. One possibility is the reduction of combustion temperature with fuel modification, e.g., water emulsion or with the humidification of the charge air. Other options include exhaust gas recirculation (EGR), the modification of the combustion process and its timing and also the treatment of the exhaust gas with selective catalytic reduction (SCR). However, the purity of water is an issue with all options that use water and the sulfur content influences many of the possibilities for emission-reduction technologies including EGR and SCR (Buhaug, 2009).

3. Extended emission estimation model (STEAM2)

In this chapter, the extended model, Ship Traffic Emission Assessment Model (STEAM2), is presented and especially the new features since the previous model are illustrated in greater detail.

Previously at the Finnish Meteorological Institute a method was presented for the evaluation of the exhaust emissions of marine traffic, based on the messages provided by the Automatic Identification System (AIS), which enable the identification, location and speed determination of ships (Jalkanen et al., 2009). The model used an internal ship database that included, among other specifications, engine power, maximum speed and weight and spatial attributes. The model was based on the relationship of the instantaneous speed to the design speed and the use of the detailed technical information of the engines. The effect of waves was also included in the model. The previously developed model was applicable for evaluating only the emissions of NO_X, SO_X and CO_2.

The main differences between the new model (STEAM2) and the previously developed one (STEAM) include that the CO- and PM emissions are included in the latter model. A new evaluation method is also used for analyzing the resistance of ships in water. The model also includes a refined modeling of the power consumption of auxiliary engines, which depend on ship type and its operation mode and also the effect of engine load to fuel consumption. An illustration of the main components of the STEAM2 model is presented in Figure 1. The main input data sources are the internal ship database and the AIS data. Based on the properties of the ships and its power requirements, the model can evaluate the power consumption and load of the engine, and then the fuel consumption of the ship. Based on these values, the model is used to evaluate the emissions of NO_X, SO_X, CO, CO_2 and PM, as a function of time and location.

3.1 Input data for the model

The automatic identification system (AIS) was introduced by the International Maritime Organization to enhance safety and efficiency of navigation, safety of life at sea and also for maritime environmental protection through better identification of vessels (Mokhtari 2007). The main objective, however, was to provide precise information that could be used to collision avoidance. AIS equipment operates on VHF frequency and

is able to detect other AIS transmitters nearby. AIS message includes static information about the identification (IMO and MMSI-number), name and ship type, dynamic information such as the position, heading and speed over ground and also voyage related information about the type of cargo and destination.

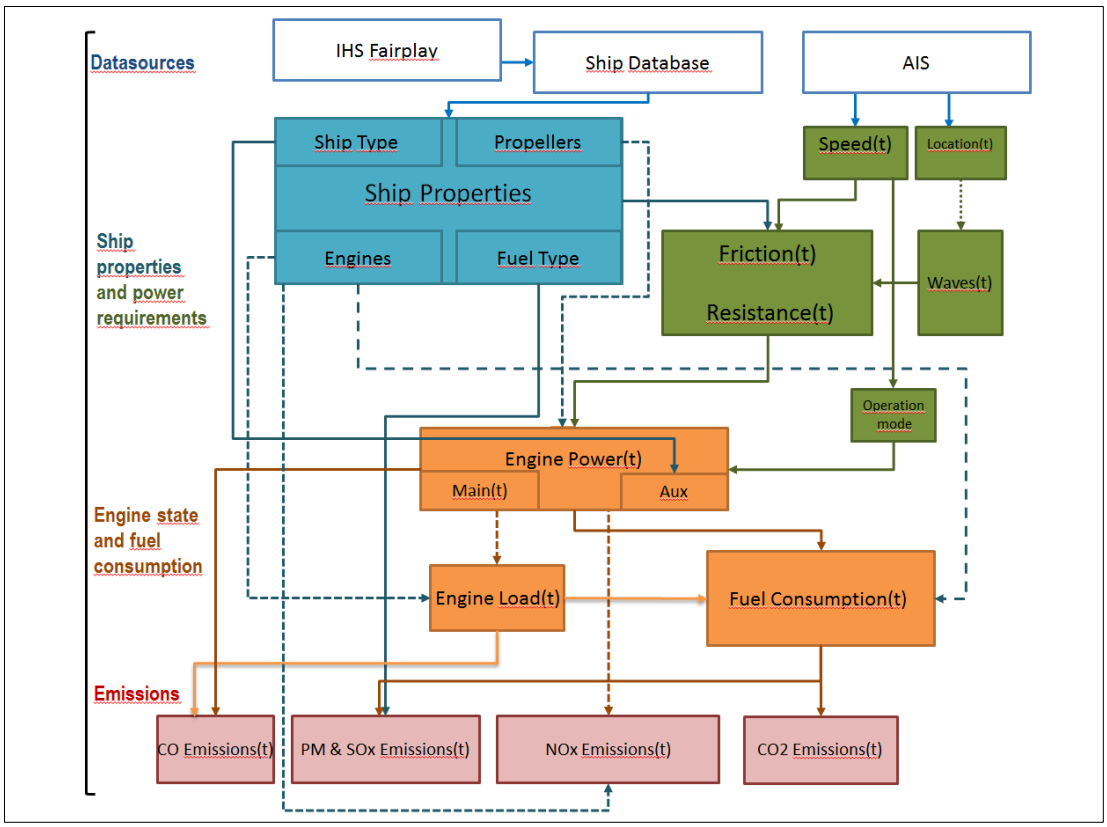

Figure 1: A schematic diagram of the main components of the STEAM2 model and their inter-relations. The model input data sources are presented on the uppermost row of rectangles, and the model output data (i.e., emissions) are presented on the lowest row of rectangles. The arrows describe either the flow of information in the model, or a modeled dependency between various factors. The different colors denote the various categories of factors included in the model; dotted and solid arrows are used only for visual clarity.

Often some of the data fields of lesser importance to the collision avoidance purposes, such as cargo type, are left blank but nevertheless the use of the AIS data facilitates an accurate mapping of the ship traffic, including the detailed instantaneous location and speed of each vessel in the considered area. For example, more than 210 million position reports were received from the 9497 AIS targets in the Baltic Sea in 2007. For ships in a regular schedule, this results in tens of thousands of position updates each month. Decrypted AIS data, usually with time interval between two consequent messages of no less than 3 minutes, is provided by Helcom for the model. Currently for

a typical month, the amount of AIS message inputs for the model amounts to more than 2 gigabytes of data and therefore, even when much more frequent AIS data would be readily available, messages with longer time interval are favored because of computational limitations.

The internal ship database of the STEAM2 model contains the technical details of ships used in the evaluation of emissions. The database contains the information of more than 30 000 ships; this is approximately a third of the global fleet. Most of the ships in the database are newer ships that have been built within the last two decades; most of these ships are frequently operating in the Baltic Sea. If ships with new IMO signature are appearing in the AIS messages, then a query is sent to HIS Fairplay and if the particular ship has been listed there, then the ship with its specifications from IHS Fairplay is added to the internal ship database before the emission estimation program is run. Especially for older ships it would be wise to update ship specifications from time to time, but due to high costs updating isn't done regularly. In case a ship sending AIS messages cannot be identified using the ship database and with queries to IHS Fairplay, then the ship is assumed to be a small tugboat vessel and the model uses generic average attributes of small tugboats for the unidentified ship.

3.2 Power and ship attribute estimation

A method presented by Hollenbach (1998) is used to calculate the resistance of ships due to moving in water. The predictions of the Hollenbach method agree well with other performance prediction methods, such as those of Holtrop-Mennen (Matulja and Dejhalla, 2007; Holtrop and Mennen, 1982; Holtrop and Mennen, 1978). The use of this method, compared with the previous model, improves the predictions of resistance and engine power, especially in cases, in which the hull dimensions and the engine data is available, but the design speed of the vessel is unknown. In the previous version of the STEAM model, the design speed was a critical parameter for the model performance; if that value was not available, an average speed was used instead that was specific for each ship type. The use of the Hollenbach method avoids such assumptions, and therefore provides a more reliable basis for the resistance calculations.

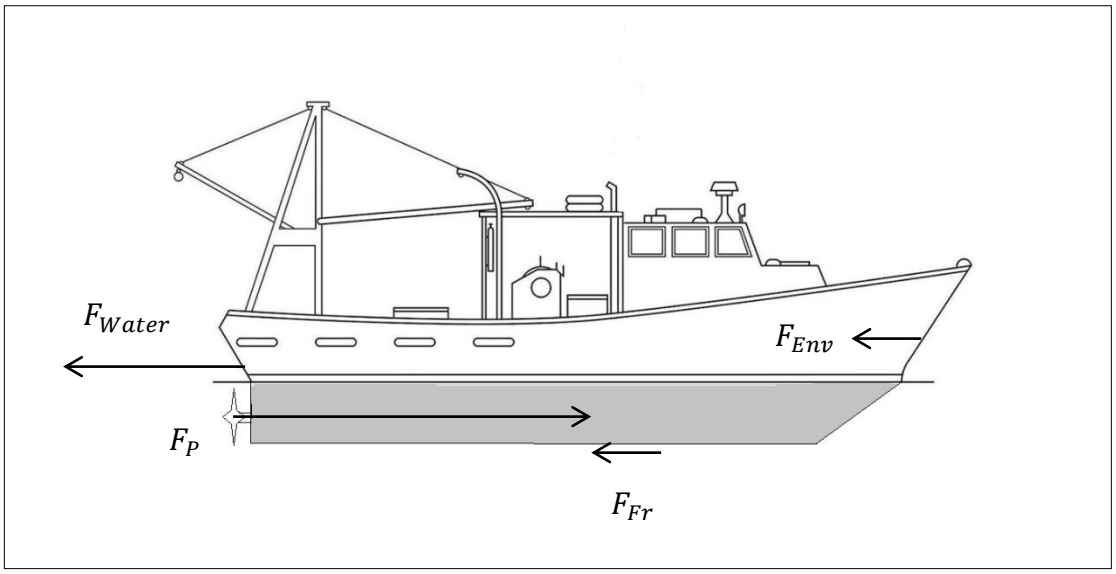

Figure 2: A marine vessel moving in water and the forces acting on it. F_P is the propelling force of the engine, F_{water} is the resistance from moving in water including the forming of waves. F_{Fr} is the friction between the wet surface of the ship and the sea. F_{Env} is the resistance force component in parallel to F_p which is caused by wind, sea ice coverage and ambient large waves.

In Figure 2, a marine vessel moving in water with constant speed and the forces acting on it are presented. Waves tend to increase the fuel consumption of ships no matter what direction the waves are propagating in relation to the ship. The model takes the effects of waves into account by using the hourly significant wave heights and the mean wave direction data from a separate wave model. Besides the sea state, the Force induced by waves depends on parameters describing the wet surface and the three-dimensional structure of the hull and also of the contact angle between the hull and waves (Jalkanen, 2009). Currently, F_{Env} is set to include only the resistance from waves because air resistance in most cases have been calculated to be miniscule compared to other forces and moving through ice coverage is yet to be implemented.

The vessel of Figure 2 is in equilibrium state as the acceleration is zero and therefore the sum of forces is also zero:

$$F_P - F_{water} - F_{Env} - F_{Fr} \approx 0 \qquad (1)$$

Where F_P is the propelling force of the engine, F_{water} is the resistance from moving in water, F_{Env} is the resistance from ambient large waves which is in parallel to F_P and

F_{Fr} is the friction of the water surface. Taking into account that $P(t) = \frac{dE}{dt} = \frac{F(t)ds}{dt} = Fv(t)$, the propelling force can be written as

$$F_P(t) = \frac{P(t)\eta_{qpc}}{v(t)} \tag{2}$$

where $P(t)$ is the current engine power, $v(t)$ is the vessel speed and η_{qpc} is the quasi propulsive constant. The dimensionless quasi propulsive constant η_d is used to describe the effectiveness of converting the main engine power to actual propelling power, taking propulsive losses arising from transmission, hull, shaft and propeller itself into account. Finally, multiplying Eq. 1 by $v(t)$ yields

$$P(t) = \frac{v(t)(F_{water} + F_{Env} + F_{Fr})}{\eta_{qpc}} \tag{3}$$

According to empirical studies of Watson (1998), η_{qpc} can be estimated indirectly from the ship attributes in the following manner:

$$\eta_{qpc} = 0.84 - \frac{RPM_{Pr}\sqrt{LBP}}{10000} \tag{4}$$

where RPM_{Pr} is the rpm of the propeller and LBP is the length between perpendiculars. The physical dependencies between efficiency, propeller rpm and LBP are quite complicated and are best left outside of this thesis. Propeller efficiency is commonly substantially less than unity; usually 60-80 % of the main engine power is transmitted to the water by the propeller (Watson, 1998).

As Eq. 4 shows, a value for propeller rpm is required to estimate the propeller and transmission losses and the required main engine power. If the number of propellers is unknown, then the ship is simply assumed to operate with a single propeller. Propeller diameter is estimated using the method described by Watson (1998). An estimate for propeller diameter d in meters is

$$d = 16.2\frac{{P_S}^{0.2}}{{RPM_{Pr}}^{0.6}} \tag{5}$$

where P_s is the service power of the main engine (80 % of the maximum continuous rating provided by IHS Fairplay (2010) in kilowatts and N is the propeller's rpm. This

method was used for all single-propeller vessels, for which the propeller rpm was known. For multi-propeller vessels, if both the propeller rpm and diameter were unknown, a value was used that is based on a fraction of vessel draught. This approach does not consider exceptional cases of surface piercing propellers. It is expected to lead to a reasonable estimate of propeller diameter. In multi-propeller cases and also if propeller data is unavailable, propeller size is estimated with a ship type specific fraction of draught, as draught is one of the main limiting factors for propeller size. These fractions of draught values have been statistically estimated using the internal ship database.

If propeller rpm cannot be determined from ship technical data and it cannot be estimated using Eq. 4 and 5, the power is predicted based on the previous version of the model (Jalkanen et al., 2009). In these cases, 80 % of the main engine power is assumed to be in use, when the vessel is traveling at its design speed. The required power is computed applying a relationship kv^3, where k is a ship-specific constant generated from main particulars and v is the instantaneous speed of the vessel.

In the internal ship database sufficient propeller details exist for about 60 % of the cases, which facilitate the evaluation of the quasi propulsive constant. In the remaining cases, the previous method (Jalkanen et al., 2009) of engine power estimation for the main engines has to be used, which requires that the design speed of the ship has to be known. In approximately five percent of the ship database entries both the propeller rpm and vessel design speed are missing. In such cases, the emission predictions are relatively less accurate, as average values specific to this ship type have to be used as a substitute for the missing ship data values. The values larger than the total installed engine power are not allowed for by the model.

3.2.1 Resistance and friction from moving in water

Modern ship designing and building has its roots dating back to the Middle Ages and because of this, even today many empirical rules of thumb involving lots of different spatial parameters and coefficients are being followed by ship builders as a first design phase. This is reflected on the Hollenbach method as well, which is used to calculate F_{water} and F_{Fr} based on the physical dimensions of the ship. The method itself is based on the resistance measurements of 433 tank tests. The application of the method, however, is in many cases limited by the availability of the hull and propeller details and

for reliable power predictions using this model, either propeller revolutions per minute (rpm) or propeller size has to be known.

The resistance from moving in water is mainly affected by a coefficient called as the block coefficient C_B, which reflects a resistance factor originating from the shape of the hull. Roughly put, more hydrodynamic hull has a smaller C_B than a bulkier one. The block coefficient cannot be obtained from commercial available databases however, and thus C_B is needed to be estimated with a method suggested by Watson and Gilfillan (1976) and further described by Townsin (1979): The Block coefficient can be written as

$$C_B = 0.7 + \frac{1}{8}\text{atan}\left(\frac{23-100\boldsymbol{F_n}}{4}\right), \tag{6}$$

where $\boldsymbol{F_n}$ is the Froude number. The Froude number is defined as the ratio of a characteristic velocity to a gravitational wave velocity or equivalently as the ratio of a body's inertia to gravitational forces. $\boldsymbol{F_n}$ It is used to determine the resistance of an object moving through water and is computed in the Hollenbach method as follows:

$$\boldsymbol{F_n} = \frac{v(t)}{\sqrt{gL_{WL}}} \tag{7}$$

Sadly, the waterline length L_{WL} in Eq. 7 isn't readily available for most of the vessels. In these cases, an approximation using the average value of overall length in meters (LOA) and length between perpendiculars in meters (LBP) is used instead. Thus, The Froude number is given by:

$$\boldsymbol{F_n}(t) = \frac{2v(t)}{\sqrt{g(LOA + LBP)}} \tag{8}$$

The residual resistance that is approximately the sum of $F_{water}$and F_{Fr} is given by:

$$F_R(t) = C_R \cdot \frac{\rho}{2} v^2(t)S \tag{9}$$

where ρ is the density of seawater and C_R is a ship specific factor, which is also speed dependent as the displacement of water caused by the ship is dependent on speed and S is the wet surface of the ship. The Hollenbach method essentially estimates C_R using hull and ship specific parameters, the block coefficient C_B and wet surface S. Using Eq.

4 and Substituting F_R given by the Hollenbach method to Eq. 3 yields the following formula for power estimation:

$$P(t) = \frac{v(t)(\alpha(\boldsymbol{F_n})C\rho v(t)^2 + F_{Wave})}{0.84 - \frac{N\sqrt{LBP}}{10000}} \quad (10)$$

where $\alpha(\boldsymbol{F_n})$ is a dimensionless function of the Froude number and C is a ship specific constant which is affected by the ship's dimensions, number of bossings and hubs, etc.

3.2.2 The evaluation of auxiliary power

Just like in the previous version of the model, the main principle of auxiliary power estimation is a classification by ship type and its operation modes. There are three different operation modes available for each ship: maneuvering near harbor areas, cruising and hoteling. The operation mode is currently being deduced from the ship's speed data. The different ship types are discussed in greater detail in Chapter 6.

In the previous model version, especially the estimation of auxiliary power was observed to be insufficient, and thus the following modifications were made: Passenger class vessels which includes cruise ships, Roll-in, Roll-off vehicle carriers (RoRo), vehicle passenger ships (RoPax) and yacht vessels use a base value of 750 kW of auxiliary engine power for all operating modes, but an additional requirement of 3 kW is added for each cabin. This emulates the additional need for electricity required by air conditioning, hot water and other electrical installations inside the cabins. For reefers and containerships, similar assumptions are applied. A base value of 750 kW is used while cruising, 1000 kW during hotelling and 1250 kW while maneuvering. In addition to these values, each refrigerated Twenty-foot Equivalent Unit (TEU, standardized cargo container) consumes approximately 4 kW of electricity to maintain the containers in a constant temperature. Clearly, the actual power requirement of the container depends on the temperature difference between the environment and the container (Wild, 2009).

All other vessel classes use 750, 1000 and 1250 kW for cruising, hotelling and maneuvering, respectively. With these modifications, STEAM2 can distinguish between large and small vessels of the same ship type. However, in all cases, the installed auxiliary engine power is used as an upper limit for the predicted auxiliary engine power (in cases, for which the computed auxiliary power would exceed the installed auxiliary

power). Boiler energy usage is included in the estimates of auxiliary engine power; these have not been modeled explicitly due to the lack of data.

3.3 Engine load and the specific fuel oil consumption (SFOC)

Instantaneous total fuel consumption is influenced by many independent factors. Fuel consumption of main engines used in propulsion is commonly estimated in available literature as a product of the constant specific fuel oil consumption (SFOC) and instantaneous engine power, which results in a linear relationship between fuel consumption and engine power. Ideally, all power systems that require fuel to operate should be modeled separately, such as the main engines for propulsion, the auxiliary engines for power generation and the boilers for heat generation. However, in practice a separate modeling of all of these is currently not feasible.

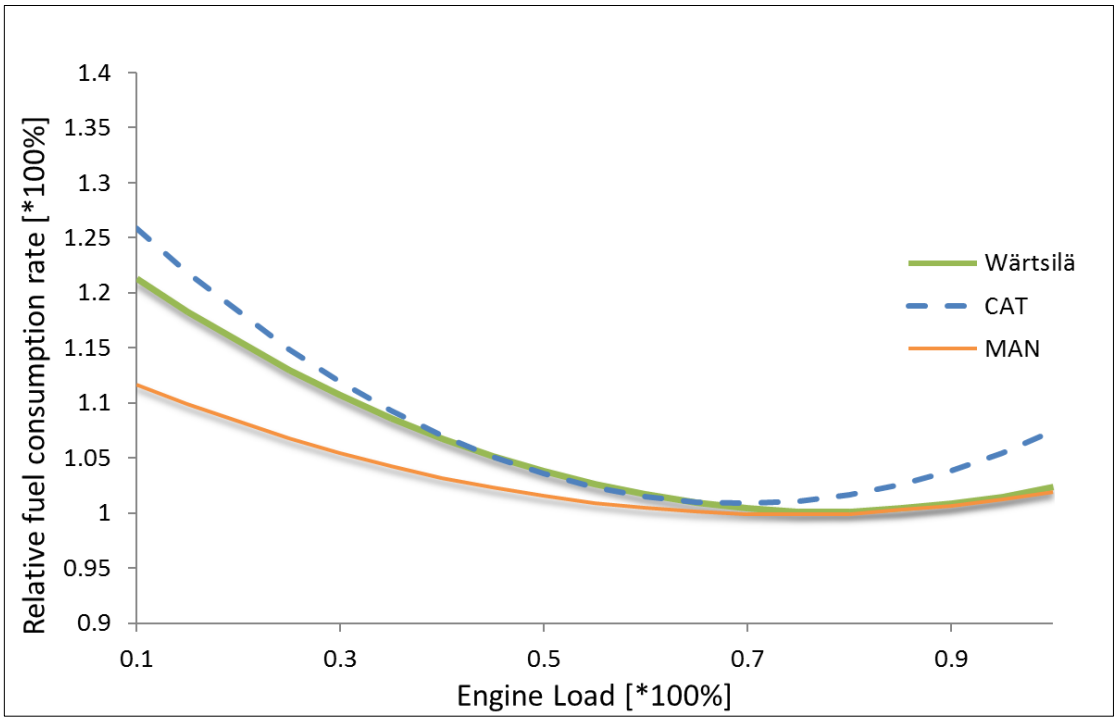

Figure 3: The relative specific fuel-oil consumption (SFOC) as a function of the relative engine load, based on the data of three engine manufacturers: Wärtsilä, Caterpillar and MAN. The data of Caterpillar is based on three different SFOC curves of small 4-stroke engines, and the data of MAN is based on large 2-stroke engines.

The relative SFOC curve provided by the engine manufacturer Wärtsilä for a medium sized 4-stroke engine is presented in Figure 3. Using SFOC studies and engine specifications (Caterpillar, 2010; Man B&W, 2010), two other relative SFOC curves by other manufacturers are also presented. The engines by MAN considered here are

large 2-stroke models, whereas the Caterpillar engines are relatively small 4-stroke models.

For all three curves presented, the SFOC is a non-linear function of engine load, and this function has a minimum at a specific engine load. For the data of Caterpillar, MAN and Wärtsilä, the minimum is approximately at the relative engine load of 70, 75 and 80%, respectively. Minimizing fuel oil consumption therefore requires engine loads approximately from 70 to 80 %. There is an approximately parabolic dependency between the SFOC and the engine load.

In the STEAM2 model, a parabolic SFOC function for all engines is assumed. Using regression analysis of the comprehensive SFOC measurement data from Wärtsilä, a second degree polynomial equation for the relative SFOC was derived:

$$SFOC_{Relative}(EL) = 0.455\,EL^2 - 0.71\,EL + 1.28 \qquad (11)$$

where EL is the engine load ranging from 0 to 1. The absolute fuel consumption is estimated from

$$SFOC(EL) = SFOC_{Relative}(EL) * SFOC_{base} \qquad (12)$$

where $SFOC_{base}$ is the so-called base value for SFOC which is a constant for each engine. According to second IMO greenhouse gas report (Buhaug et al., 2009), a lower consumption is assigned for new engines, describing the technical development and better efficiency of modern engines. The base value is also influenced by engine stroke type and power. Primarily, the engine-model specific base values for SFOC from the engine manufacturers are used but in case such a value is not available, the value is evaluated (taking the above mentioned factors into account) according to the IMO GHG2 report (Buhaug et al., 2009). Depending on the stroke type, age and power rating of the engine, the base SFOC value typically ranges between 170g/kWh and 220g/kWh.

For simplicity, it has been assumed that engine load and SFOC dependence from Equation 11 applies to all engines. For turbine machinery, $SFOC_{base}$ of 260 g/kWh is used. Auxiliary engine $SFOC_{base}$ was set to 220 g/kWh and the same load dependency was applied.

In some ships, a diesel-electric engine setup has been installed, in which a diesel engine is used to generate electricity for auxiliary engines and also for electric motors to drive the propellers without any mechanical contact. The main engine is usually operating constantly on an optimal engine load state, which can be regarded as one of the most notable advantages of diesel-electric setups over traditional marine diesel engines. Thus, the optimal SFOC value is assumed for every diesel-electric setup in the model.

3.4 Multi-engine installations

While it is straightforward to estimate an engine load of a single engine ship, if required power is known, this estimation is more challenging for multi-engine setups, which are common especially among passenger ships. Therefore, a load balancing scheme for multi-engine installations has also been implemented in the STEAM2 model.

Load balancing is a crucial issue for the proper functioning of multi-engine installations. Engines that are not needed at a specific moment can be turned off, which saves fuel and ensures that the remaining engines are operated with an optimal engine load. To simulate this operation of the engines, the STEAM2 model determines the minimum number of engines, which need to be in operation to overcome the predicted resistance of the ship. The model assumes all main engines to be identical, a minimum number of engines are assumed to be used, and the load values are assumed to be less or equal than 85 %. The latter assumption is needed, as engine loads larger than 85% are commonly avoided. If this load values would be exceeded, an additional engine is assumed to be taken online and the load is balanced among the operational engines. For example, let us consider a ship with four installed engines, each with a power of 6000 kW, and an instantaneous power requirement of 11000 kW. The minimum requirement to obtain 11000 kW would require operation of two engines at 91.7% load level, which is not feasible. The modeling assumption is therefore that three engines would be used instead, each with a load of 61.1%.

A limitation of this approach is that the model treats all main engines as equal and neglects engine setups, for which one engine in a pair is larger than another. For instance, in case of four engines with two pairs of identical engines, a so-called 2+2 setup, the accuracy of the predictions of fuel consumption and emissions will deteriorate. Passenger classed ships are required to have at least two engines operational at all times, due to chief engineer interviews and vessel safety rules. Load balancing is

applied to both main and auxiliary engines, but in case of diesel-electric engine setups, all the power commonly required for ship systems and propulsion are taken from the main engines.

3.5 Exhaust emissions modelling

Using the estimates for current instantaneous power, fuel consumption and ship attributes taken from ship database, emissions of every emission type presented in Chapter 2 are estimated for ship routes derived from the AIS data. Ship routes are generated from the sequence of coordinates simply using a linear interpolation between consecutive coordinates for each ship with unique identification signature. The main aim is that the model provides accurate emission factors for the all pollutants, including all the chemical components of PM, for all values of the fuel sulphur content and the engine load. The evaluation of the influence of engine load is needed especially for an accurate description of emissions of PM, SO_X, CO and CO_2. All emissions have therefore been assumed to be dependent on engine load, except for those of NO_X.

3.5.1 NO_x emission factor

Besides high temperature, the amount of combusted nitrogen is strongly dependent on time allowed for combustion reaction, and thus is affected directly by the RPM value of the engine. Therefore, high speed engines produce less NO_X emissions per kWh than low speed engines as the duration of high temperature phase is shorter. In several studies it has been concluded that NO_X emissions are not strongly affected by fuel consumption and thus are left independent of SFOC in the model.

NO_X emissions are calculated in the model using a fixed emission factor [g/kWh], which is determined by the main engine's rated speed (RPM) value using the NO_X emission factor curve from IMO (Tier I), which reflects the current limits for the allowed NO_X emission factors as a function of engine's rated speed. In the forthcoming years, however, marine vessels are expected to meet even lower emission factor limits (given by Tier II and Tier III curves) than the model assumes. These three emission factor limits as a function of RPM are presented in Figure 4.

As the three NO_X emission curves in Figure 4 illustrates, NO_X emissions tend to increase significantly in the lower RPM regime. A typical 4-stroke engine has an RPM

of more than 500 revolutions per minute while it is not uncommon that a powerful 2-stroke engine is running slower than 100 revolutions per minute.

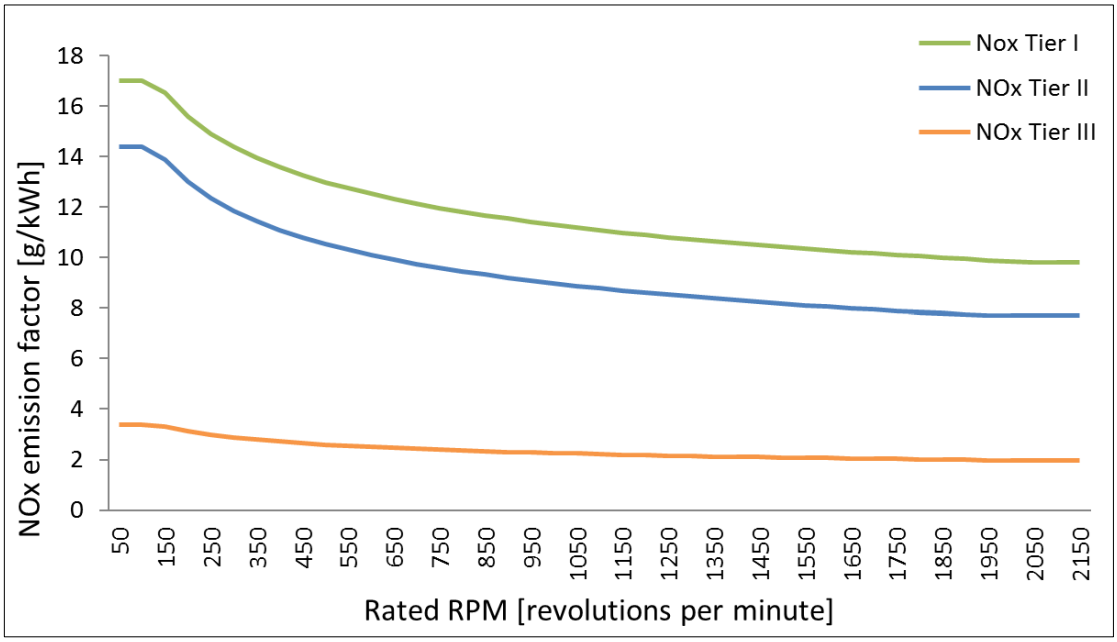

Figure 4: NO_X Emission Limits set by MARPOL Annex VI. The upper curve (Tier I), since January 2000, applies retroactively to all engines with power more than 150kW. Curve in the middle (Tier II), applies after January 2011. The third curve (Tier III), which applies only for SECA areas, comes into effect on January 2016.

Starting from January 2011, Tier II standards are expected to be met by combustion process optimization for each new ship. Most of the engine manufacturers, however, have been producing Tier II compliant engines in anticipation of the Tier II limitations for the last decade. It is not likely that an engine has significantly lower NO_X emission factor without having some abatement method installed, which in that case would be specified in the ship database and taken into account. Moreover, for each new ship, the engine's NO_X emission factor is certified (with ISO-8178 test) to agree with the IMO Tier II curve. Thus, the maximum allowed value for NO_X emission factor given by Tier II curve can be applied for new ships with reasonably good accuracy, although with a slight possible overestimation.

3.5.2 PM emission factor

As discussed previously, fuel consumption is dependent on engine load and thus the emissions of several pollutants have the same dependency. If the engine is run outside its normal operating load range, fuel consumption and thus also emissions are increased, since the engines are not commonly optimized to run on low loads for

prolonged periods. In case of multi-engine setups, however, unnecessary engines can be turned off to gain better efficiency in fuel consumption as it was discussed in Chapter 3.3.

Several authors have reported experimental results on the composition of particulate matter as a function of engine load (Agrawal et al., 2008; Agrawal et al., 2010; Petzold et al., 2008; Moldanova et al., 2009; Sarvi et al., 2008) and sulphur content (Sarvi et al., 2008; Buhaug et al., 2009) and this relationship between PM emissions, engine load and sulphur content has been implemented into the model.

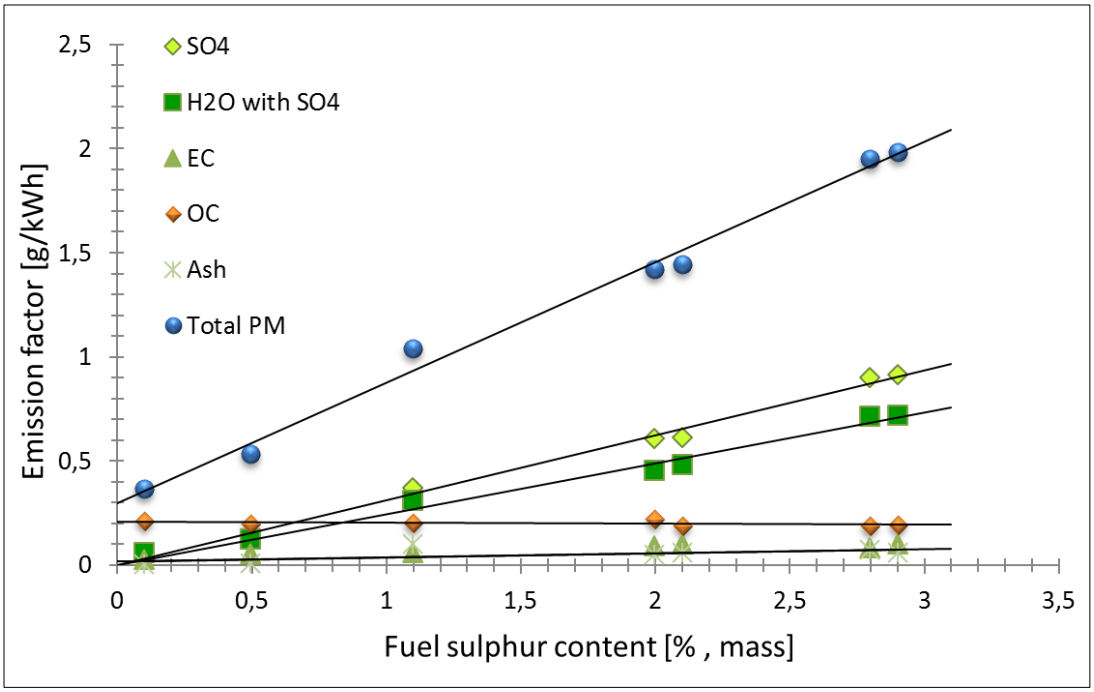

Figure 5: The emission factor of the total PM, and for its chemical constituents as a function of fuel sulphur content (mass-based percentage), based on the data from the second IMO GHG study (Buhaug et al., 2009). Linear regression curves are presented as black lines. The emission factors of the total PM, SO_4 and H_2O are linearly dependent on the fuel sulphur content. The data points for EC and ash are partly overlapping in the figure.

The sulphur content of the fuel has a crucial influence on the PM emissions. The dependency of PM emission factor on fuel sulphur content was modeled according to Buhaug et al. (2009), as presented in Figure 5. As expected, the emission factors of the total PM, SO_X and its associated water molecules are linearly dependent on the fuel sulphur content, whereas the emission factors of EC, OC and ash are almost totally independent of this factor. The emissions of PM could therefore not be eradicated

totally, even if sulphur would be completely eliminated from ship fuels (Winnes and Fridell, 2010; Buhaug et al., 2009).

Applying linear regression analysis to the data presented in Figure 5 yields the following emission factor dependencies:

$$EF_{SO_4}(S) = 0.312\,S \qquad (13a)$$
$$EF_{H_2O}(S) = 0.244\,S$$

and

$$EF_{EC} = 0.082\ g/kWh,\ EF_{OC} = 0.20\ g/kWh, \qquad (13b)$$
$$EF_{Ash} = 0.06\ \text{g/kWh}$$

where S is the fuel sulphur content in mass percentages and the emission coefficients for EC, OC and ash have been assumed to be independent of the sulphur content. However, the amount of ash may change between different fuel grades. Comparing the atomic masses of SO_4 and its associated water in Eq. 13a implies that each SO_4 molecule is associated with approximately 4.2 molecules of H_2O according to the IMO GHG study. The total PM emission factor (in g/kWh) is assumed to be the sum of the above mentioned emission factors:

$$EF_{PM2.5}(S) = (0.312 + 0.244\ )S + 0.3 \qquad (14)$$

In STEAM2, the PM emissions [g/kWh] are evaluated as the product of specific fuel-oil consumption and emission factors. For example, the total PM emission as a function of engine load and fuel sulphur content is

$$TotalPM(EL,S) = SFOC_{relative}(EL) * EF_{PM2.5}(S) \qquad (15)$$

where the relative $SFOC$ is computed using Eq. 11. The variations of this emission factor have been graphically illustrated in Figure 6. In short, the variation of the PM emission factor for different components has been modeled based on the variation of SFOC. The emissions of all PM components are modelled based on the variations of SFOC and instantaneous power, and in addition the emission factors of sulphate and associated water are dependent also on the fuel sulphur content.

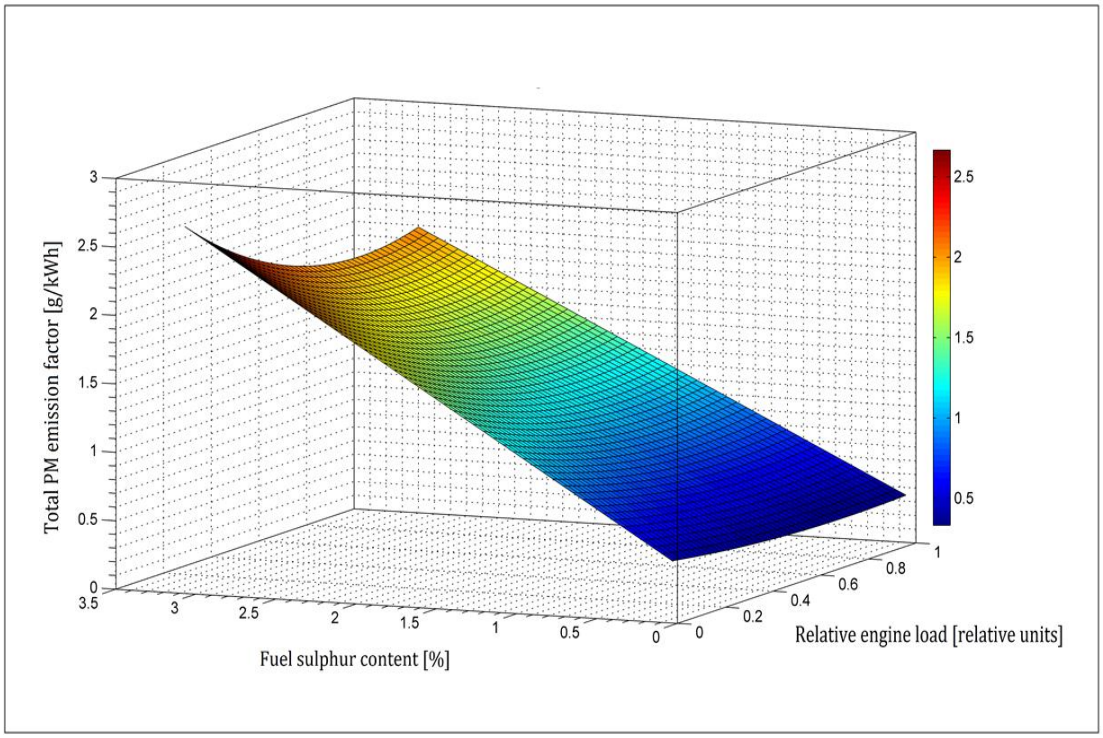

Figure 6: The predictions of the STEAM2 model for total PM emission factor [legend, in units of g/kWh] as a function of engine load and fuel sulphur content.

It was concluded that the behavior of one of the PM constituents behave differently with very low engine loads. In two separate studies made by Agrawal (Agrawal, 2008) and Petzold (Petzold, 2008) emission factor for OC was observed to increase up to 0.6g/kWh with very low engine loads. Such an increase was not explained through the increase in SFOC as the other components in the studies were not affected by low engine loads nearly as much. Thus, it was concluded that OC emissions are depended on engine load with very low engine loads. Based on these measurements using regression analysis, as a special rule, the emission factor for OC was set to equal

$$EF_{OC} = \begin{cases} 0.2\,, & EL \geq 0.25 \\ 1.35e^{-7.6EL}\,, & 0.15 < EL < 0.25 \\ 0.6\,, & EL \leq 0.15 \end{cases} \quad (16)$$

OC emissions are effectively multiplied with low engine loads through the combination of SFOC increase and Eq. 16, although it should be highly uncommon for any large ship to be sailing with such a low engine load for economic reasons.

3.5.3 SO_x emission factor

SO_X emissions originate from the residual sulphur of the combusted fuel and thus the emission factor for SO_X depends mainly on the current fuel consumption and therefore is affected by engine load as presented in Chapter 3.3.

All of the sulphur molecules in fuel is assumed to be converted either to sulphate (SO_4) or sulphur oxides (SO_2, SO_3). The amount of SO_X is calculated the conservation of matter –principle: The amount of sulphur in grams m_S for any consumed fuel amount must satisfy

$$a * m_{SO_X} + b * m_{SO_4} = m_S \tag{17}$$

where coefficients a and b are the relative sulfur-mass content of the particles. One sulphur atom weights $32.06u$. The ratio of SO_2 and SO_3 particles is assumed to be one and thus the average mass ofSO_X is $72.06u$. Using the atomic mass of 96 for sulphate, the coefficient a is calculated to equal 0.444 and b is equal to 0.333. For any fuel consumption [g/kWh] the amount of sulphur per kWh is $\frac{S*SFOC}{100}$ and thus, combining Eq. 17 and 13a yields

$$m_{SO_X} = \frac{\frac{S * SFOC}{100} - 0.333 m_{SO_4}}{0.444} \tag{18}$$

The amount of sulphate depends on S and SFOC as well and thus the ratio of $m(SO_X)$ and m_{SO_4} is constant. It can be calculated that for any given SFOC the model uses the following ratio:

$$\frac{m_{SO_X}}{m_{SO_4}} = 12.8 \tag{19}$$

Taking into account the atomic weights of SO_4 and SO_X, Eq. 19 can be presented in an equivalent form using the conversion ratios, yielding the following conversion rate for sulphate:

$$\left(\frac{dN_{SO_4}}{dt}\right)\left(\frac{dN_{SO_X}}{dt}\right)^{-1} = \frac{0.333m(SO_4)}{0.444m(SO_X)} = 5.5\% \quad (20)$$

where $\frac{dN_{SO_X}}{dt}$ is the number of converted particles per time unit and the conversion rate is assumed to be constant. According to the model then, for every sulphate molecule there is approximately 18 SO_X particles formed simultaneously.

3.5.4 CO_2 and CO emissions modeling

Assuming perfect combustion conditions, the amount of emitted CO_2 can be estimated in a straightforward manner from the amount of fuel burned. However, the CO emissions are substantially more dependent on engine load. The data based on three experimental studies and the modeled dependency of the base emission factor of CO as a function of engine load has been presented in Figure 7. The CO base emission factor as described by Sarvi et al. has been adopted in STEAM2.

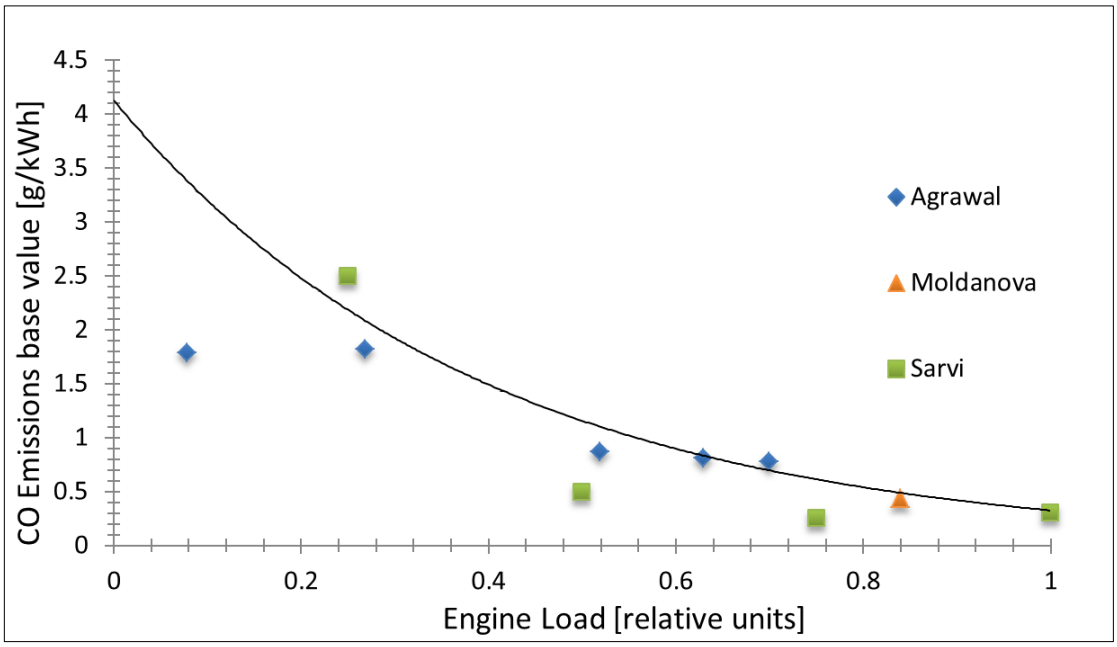

Figure 7: The base value of CO emission as a function of relative engine load. The measurements of Agrawal, Moldanova and Sarvi have been shown, and the CO base emission factor curve is based on Sarvi. The emissions of CO are also influenced by rapid changes of relative engine load.

During normal engine operation, when engine load ranges from 75% to full load, the base emission factor of CO is below 0.75 g/kWh according to Sarvi (2008). However, using the engine at low engine loads will significantly increase the CO emission factor.

Moreover, a rapid change of engine load has been observed (Cooper, 2003; Cooper, 2001) to result in significantly increased emissions of carbon monoxide. This is usually the case, when the ship is accelerating or actively decelerating (braking). Therefore, the modelled curve (as presented above) has been modified with an additional scaling term, which amplifies the CO emission factor, if the ship is accelerating.

Using this scaling factor called Acceleration Based Component (ABC), the CO emissions takes the following form:

$$EF_{CO} = CO_{base}\, ABC \tag{21}$$

where

$$ABC = \max\{\alpha \frac{|\Delta v|}{\Delta t}, 1\} \tag{22}$$

For simplicity, the empirical factor α has been assumed to be the same for all ships, α = 600. The ABC is 1.0, if there is no significant acceleration; otherwise it is larger than unity. Strictly speaking the ABC value should be ship-dependent. More experimental data would be needed to model these relationships in more detail. Moreover, the modeling above cannot distinguish between natural deceleration (engines stopped) and active braking (ship using its engines to decelerate). Therefore, the CO emissions might be over-predicted in case of natural deceleration. In the following chapter, the ABC factor for CO emissions is discussed in greater detail.

4. Further improvements for the extended model version

In order to estimate emissions correctly and associate them with correct geographical areas, (i) ships are needed to be identified and associated with correct specifications, (ii) the instantaneous power is needed to be estimated correctly and (iii), the emission formation processes are needed to be modeled correctly using the derived fuel consumption and engine state. It is not surprising that such a model is susceptible to host of different sources of error as none of the three procedures i-iii is easy to execute with high precision.

Even though the prediction accuracy of the model has been observed to be satisfactory (Chapter 5), it can be made better and more consistent. Therefore the model and its features have been under re-evaluation. Sources of error have been identified and also totally new features are planned to be implemented as several of these have been estimated to have a significant impact on emission estimates and prediction error. These potential sources of error, shortcomings and new possible features are discussed in this chapter.

4.1 Currents

The Baltic Sea has regular currents and streams throughout the year, even though the strength of these currents may not be comparable with those of the Atlantic or North Sea. The speed of these water flows, however, is large enough to affect the power estimates significantly. The whereabouts of the most notable currents in the Baltic Sea are presented In Figure 8.

In order to take the effect of the current into account, the speed of the vessel in relation to flowing water is needed to be known. For a ship sailing in a massive water flow in Figure 8, the velocity of the vessel $\mathbf{v}$ can be estimated to be the sum of current's velocity $\mathbf{v}_C$ and the ship's velocity relative to the water $\mathbf{v}'$:

$$\mathbf{v} = \mathbf{v}' + \mathbf{v}_C \tag{23}$$

If the speed of the current compared to the ship's speed is small, or if $sin\,\theta$ is small, then $\mathbf{v}'$ and $\mathbf{v}$ are almost in parallel and

$$|\mathbf{v}| \approx |\mathbf{v}'| + v_{CP} \tag{24}$$

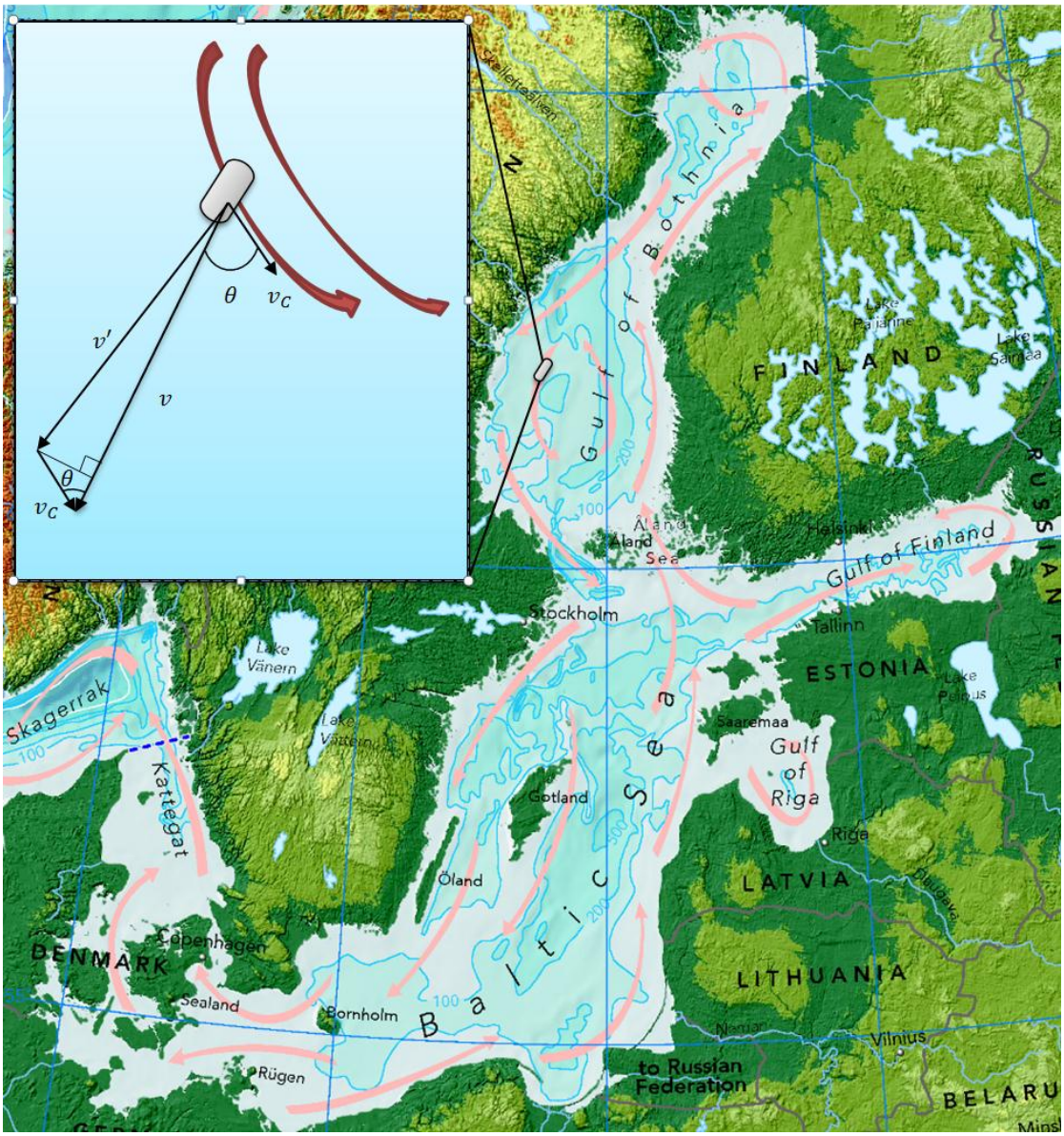

Figure 8: Major sea currents in the Baltic Sea. The sea currents and their direction are presented by red arrows. In the picture, a marine vessel with a GPS-measured speed of v is moving in current. v_c is the speed vector of the current and θ is the angle between v and v_c. The map (back picture) is provided by the European Environment Agency.

where v_{CP} is the parallel speed component of v_c in relation to **v** (and approximately to **v**' as well). the effective strength of the current is the scalar projection of $\mathbf{v_c}$ onto **v**, given by:

$$v_{CP} = \frac{\mathbf{v} \cdot \mathbf{v_c}}{|\mathbf{v}|} = \cos(\theta)\,|\mathbf{v_c}| \tag{25}$$

where θ is the angle between the ship's and the current's velocities. The angle θ can be calculated using the heading information $(0° - 360°)$ of the ship given by the AIS-

message. Thus, the speed caused by engine use v' can be calculated with the speed and heading information from the AIS data for any given $\mathbf{v_C}$.

Most of the notable currents at the Baltic Sea flow with a speed of no more than 0.25 meters per second, while the strongest currents in between Oland and Bornholm are flowing with a speed around 0.5 m/s heading towards Denmark. In Chapter 3.2, it was shown that the current engine power is strongly affected by the speed: $P \approx kv^3$ where k is some ship specific constant. Therefore, the relative effect of the addition of currents to the model estimates is

$$\frac{\Delta P}{P} = \frac{kv'^3 - kv^3}{kv^3} = \frac{v'^3 - v^3}{v^3} \tag{26}$$

Using Eq. 26 reveals, for example, that if a ship with a typical speed of 9 m/s is moving in parallel against a strong current of 0.5 m/s, then the power estimate would be increased by 17.6% by the addition of currents. The currents in other sea regions, for example, at the North Sea are much stronger and the speed of water flow may rise up to 1 m/s. For a ship with a speed of 9 m/s sailing head-on against such a strong current, the power consumption could be up to 37% more due to currents than is currently estimated. Indeed, in an unpublished study, for a large RoPax vessel sailing from Rotterdam to Harwich in September 2009, the model was seen to produce significantly biased estimates while the ship was sailing near known currents. In this study, while the engine load was kept constant the speed of the ship gradually increased for more than 1.5 m/s.

The major ship routes in the Baltic Sea seem to coincide with the most notable currents, which can be seen comparing Figure 8 and Figure 20a-b in Chapter 6. Indeed, strong currents are systematically taken advantage of by seasoned navigators. Thus it is likely that significant corrections to estimated power might be applied frequently by the addition of currents and also that the net effect on the power estimates would be negative in terms of average power. With other sea regions, however, the possibilities for taking advantage of the currents are not so simple. For example, avoiding currents of the English Channel by selecting another route is not always economically feasible.

4.1.1 Implementing the effect of sea currents to the model

As it was shown, it becomes increasingly important to take possible currents into account if the model is to be used in other, more turbulent sea regions such as the North Sea. The implementation would be fairly simple – All that is needed is a grid map of the sea region that contains the information about the speed and the direction of the current.

In the power estimation phase, the strength of currents at the location of the ship is evaluated each time. In case a strong current exists, the effective strength of the current v_{CP} is then calculated using Eq. 25. Then, the power is calculated using a corrected speed estimate v' instead of v.

With other sea regions, however, the implementation of sea currents might be more complicated as the flow of the water masses is affected by tides and changes in temperature and thus is showing a temporal dependency. Because of this, at least separate current maps for each season might be needed.

4.2 Kinetic energy and acceleration

Fuel consumption has been underestimated with the model especially near harbor areas and one known reason for this is the lack of kinetic energy modeling. The harbor areas are naturally the most important areas for the emission estimation as these are the emissions that cause most of the health problems to the general population.

Not only does the increase in kinetic energy require substantial increase in instantaneous power output for any massive marine vessel, also the ships tend to decelerate near the destination port using engine power to be able maneuver safely. Even though the effect of this addition on the estimated power curve profile near harbor areas might prove to be substantial, the total effect on fuel consumption should be nevertheless small.

Besides the force that is needed to overcome the resistance of water, the extra thrust force that causes the ship to accelerate is equal to

$$F_{+}(t) = \frac{ma(t)}{\eta_{qpc}} \tag{27}$$

where η_{qpc} is the quasi-propulsive constant of the ship. Instantaneous extra engine power $P_+(t)$ is also equal to the increase rate of kinetic energy:

$$P_+(t) = \frac{dE}{dt} \tag{28}$$

where $dE = F_+(t)\, ds$. Therefore, the extra power that is required for acceleration is

$$P_+(t) = F_+(t)\frac{ds}{dt} = F(t)v(t) \Rightarrow P_+(t) = \frac{ma(t)v(t)}{\eta_{qpc}} \tag{29}$$

If $a(t)$ is negative which is the case when the ship is decelerating the ship might be actively breaking using additional engine power. For this reason, the effective acceleration $a_{eff}(t)$, which is the result of active engine use, needs to be defined.

Effective acceleration is simply equal to acceleration if $a(t) > 0$. On the other hand, if the ship is decelerating, then

$$\begin{cases} -\frac{F_R(t)}{m} = a_{nat}(t), & \text{(30a)} \\ a_{eff}(t) = \max\{0, -a(t) + a_{nat}(t)\}, \quad a_{eff}(t) < 0, & \text{(30b)} \end{cases}$$

where $F_R(t)$ is the total resistance from moving in water and mass m is the sum of the ship's gross tonnage and deadweight. Combining Eq. 30a and 30b, the effective acceleration can be presented in the following form:

$$a_{eff}(t) = \begin{cases} \max\left(0, \frac{-F_R(t)}{m} - a(t)\right), a(t) < 0 \\ a(t), \qquad\qquad a(t) \geq 0 \end{cases} \tag{31}$$

It is not uncommon for large ships to accelerate up to a speed of 9 m/s being still relatively close to harbor area. For example, if such a vessel would happen to weight a typical amount of 60 000 tons with a η_{qpc} value of 0.7, the acceleration would require more than 1100kWh of energy. Indeed, during acceleration significant spikes have been observed in power measurements taken onboard several vessels.

4.2.1 Engine power estimates with acceleration near harbor area

The effect of adding kinetic energy to the model was tested in principle by generating acceleration values using speed and time data and adding $P_+(t)$ to the power estimatation phase in the model. In Figure 9 estimated power profiles with and without $P_+(t)$ for a Roll on/Roll off vehicle carrier ship (RoRo) arriving at a harbor in May 2010 are presented. During 14:30 – 19:00 the ship is relatively close to human population and the effect of acceleration seems to be notable during that time. Two points of active braking in can be identified near 14:40 and more notably near 15:10 but the resulting power spikes are relatively small, however.

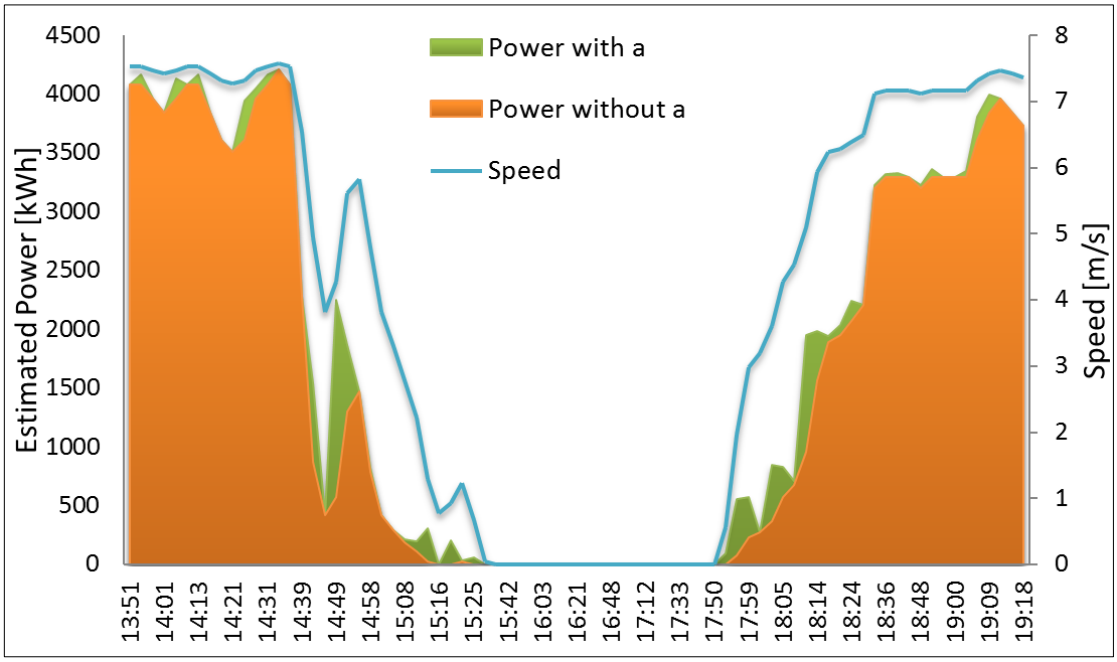

Figure 9: The predictions of the model with (green surface) and without (orange surface) acceleration based power component. The data is from a RoRo class ship sailing near harbor area in May 2010. Smoothed speed data is presented with an orange curve.

The speed curve presented in Figure 9 is a smoothed average: $v_i' = \frac{1}{2}(v_i + v_{i+1})$ for each time interval because using either end point value for the whole interpolation route might result in substantial under- or overestimation of fuel consumption during rapid speed changes. Also, the average value is needed to estimate $P_+(t)$ accurately. For example, using the current speed value in Eq. 29 for a ship which has accelerated to any speed from a total halt during a single message interval (which happens occasionally) would result in zero $P_+(t)$.

At first when the addition of kinetic energy modeling was being tested, a small number of power spikes of abnormal height were produced. Investigation revealed that the acceleration calculations for these spikes were all based on messages with time interval of mere seconds while the usual time interval was a couple of minutes. Most of these messages implied impossibly rapid speed changes to have occurred during the trip. Based on these experiments with acceleration data it was observed that filtering these kinds of "false messages" out of the input data, if possible, would result in better input data quality. In Chapter 4.4, the quality issues of the input data are discussed in greater detail.

The effect of adding kinetic energy to original power estimates was also tested against measured power consumption values. This resulted in an 4% increase in total fuel consumption which was originally underestimated for slightly more than 9%. Still, not all of the most significant measured power spikes near harbor areas were succesfully predicted. It was concluded that there was some source of systematic error of greater importance in the predictions. One of the un-modeled interactions acting on the ship that could cause such variations in speed while the engine load was kept steady according to direct engine load measurements taken onboard is the sea currents. Indeed, while the most substantial estimation bias was observed the ship was sailing against a significant sea current at the time according to a static current mapping for the Baltic Sea.

4.3 Acceleration based component for carbon monoxide emission estimation

Rapid engine load changes have been measured to cause extremely high emission spikes in contrast to steady engine load emissions. To account for such notable emission spikes, an acceleration based component to CO emission factor was introduced in Chapter 3.5. The main principle of this method was to associate high absolute values of acceleration directly with CO emission spikes. However, the presented method with a constant scaling factor which is to be used with every kind of ship may be too simplistic. Furthermore, the presented ABC factor is not able to identify active braking and thus the ABC factor may be applied when the ship is decelerating naturally.

The main assumption of the ABC factor can still be assumed to hold: CO emissions seem to be approximately linearly dependent on the rate of engine load change. Therefore the scaling factor ABC_{CO} can be assumed to be a linear function of the rate of engine load change, given by:

$$ABC_{CO} \sim \frac{EL_2(t) - EL_1(t)}{\Delta t} \tag{32}$$

Rapid engine loads and CO emission spikes have been observed to coincide only during acceleration and without acceleration the engine load is usually kept steady for economic reasons. Therefore, the engine load change in Eq. 32 can be associated with the increase in power due to acceleration. Now, let the engine load change from EL_1 to EL_2 due to an increase in the instantaneous power, which is causing the ship to accelerate. Then,

$$\begin{aligned} EL_2 - EL_1 &= \frac{P_2(t)}{P_{max}} - \frac{P_1(t)}{P_{max}} = \frac{P_+(t)}{P_{max}} \\ &= \frac{ma_{eff}(t)v(t)}{P_{max}\eta_{qpc}} \end{aligned} \tag{33}$$

where a_{eff} is given by Eq. 31. According to Eq. 32 the scaling factor should be linearly dependent on speed, acceleration and on the inverse of the acceleration duration - Three variables instead of just the acceleration of the ship. For any ship, the revised ABC factor should be defined as follows:

$$ABC_{CO} = max\{1, \frac{a_{eff}v}{\Delta t} * b\} \tag{34}$$

where b is a ship specific constant $b = \frac{m}{P_{max}*\eta_{qpc}} * c$ and c is some constant scaling factor, which might depend on the other engine specifications and it's condition. Naturally, the engine and its condition play an important role in the way how rapid engine load changes would affect emissions, but this effect is difficult to model without very specific information about the engine. Nevertheless, the ABC factor which in the extended model is based on a single case-study and disregards many of the physical factors, should at least take into account the current velocity and the time interval between the two AIS messages. Given enough measurement data, a set of coefficients b

could be identified and applied for different ship types and engine classes, resulting in much more reliable basis for CO emission spikes estimation.

4.4 The quality issues of AIS data

During the last few years, it has become apparent that not all received AIS data is relevant for total emissions estimation, or even valid information about moving ships. On the contrary, AIS data seem to contain large amount of noise, for example, unidentified ships sending messages nowhere near any ocean surface and then just a few minutes later, the same ship might be sending the another message thousand kilometers away from the initial coordinates. One reason for these kinds of incidents is that some small vessels are sending AIS messages with wrongfully calibrated transmitter. Other explanations are still under investigation.

Other concern with the emission estimation perspective is that more and more small vessels are installing AIS transmitters. Although this offers an opportunity to model even greater a share of the marine activity, the majority of these vessels cannot be identified using the internal ship database, or any other commercial information source for that matter. Therefore, preset small vessel specifications have to be used for these ships when emissions are being estimated.

4.4.1 AIS data processing

To prevent invalid AIS messages from causing imaginary routes and therefore causing overestimated and geographically biased estimates, the model needs to validate the messages that are used for emission estimation.

Previously the model performed such validity checks for every data point as a final phase for the emission estimation. Because of way the model was programmed, the only possibility to perform this kind of check in the emission estimates phase, was to compare spatial separation, speed and time interval to the next node. Based on the test, emissions are estimated from initial point to the next or are discarded. However, this test cannot be fully trusted, because it is not possible to determine the validity of a message based on the next message; for all we know the next message might be invalid and not the other way around. Also, usually the route interpolation process should be performed from point A to point C if the data for the point B is evaluated to be invalid. Even if the invalid messages were discarded correctly by the model, they are still able to cause unnecessary calculations and files to be created during the previous phases.

Indeed, the interpolation and plausibility checking process is currently vulnerable and because of this, for example, some yacht with MMSI code 0 was reported to travel several million kilometers in each month between January and May of 2006, which is of course an impossible feat for any marine vessel. Fortunately, later investigation proved that these abnormal travel distances hasn't distorted the actual emission estimates but rather are causing the ship's cumulative travel counter to build up in some cases.

Especially for the new features, the programming logic of the model posed several difficulties: When the model was programmed the emission estimation phase was viewed as a separate phase. For each data point, engine power was estimated and later on the engine power estimate is applied for the next interpolated route. Because of this, the next data point is not accessible when engine power is estimated. Hence it was impossible to deduce, for example, if the ship is accelerating or actively using engine power for braking. The solution for overcoming the presented challenges was simply, that all of the input data is to be filtered from all of the invalid ones before the processed input data is fed to the model. After appropriate filtering it is then possible, among other things, to calculate and add acceleration to the input data. Another solution would've been to make drastic technical changes in the programming code itself but would've required a lot of programming effort.

Finally, a sub program was programmed to perform various tasks, such as:

- To Sort the AIS data by MMSI code and then arrange messages by time for each unique MMSI code.
- To perform validity checks using 3 consecutive messages at a time. Based on pair-wise time separation, spatial distance and speed -check, trash messages are separate. In the speed check, calculated speed between the two consecutive ship locations is compared to the maximum speed value provided by the internal ship database.
- To filter ships with only one message sent are discarded as no route can be interpolated.
- To calculate and add acceleration based on two valid data points with the same MMSI identification.

- To provide average speed for two consecutive valid points (Needed for the estimation of kinetic energy and also for overall lag-reduction in the estimated power)

The introduction of reliable input data with acceleration offers new possibilities for the model as well as an easy way to gain control over the input data. For example, the maneuvering and the use of thrusters in harbor areas could be identified. Previously such maneuvering tests would've been impossible to perform in the power estimation phase.

4.4.2 Inactive unidentified ships

In Table 1, statistics about the AIS data for the recent years is presented. The number of messages per year has been steadily increasing while the number of different ships sending these messages is increasing even more rapidly – the number of different ships encountered in the AIS data has more than doubled between 2006 and 2010. One might assume that marine traffic in terms of travel amounts and fuel consumption in the Baltic Sea has been increasing significantly as well but this is not the case as it turns out in chapter 6.

Table 1: Annual statistics of the archived AIS messages and the annual amount of active ships. Active ship refers to a true, fuel consuming ship while all ships is the number of total ships encountered in the annual AIS data. Active IMO ships represent the regular and certified ship traffic. For ships without IMO number, no reliable commercial specification data has been available and are thus assumed to be small vessels.

Year	Archived messages	Temporal AIS coverage	Active ships (All ships)	Active IMO ships	Active ships without IMO number
2006	>171 966 000	93.36%	8160 (10810)	6851 (84.0%)	1309 (16.0%)
2007	>210 345 000	97.90 %	9326 (11780)	7355 (78.9%)	1971 (21.1%)
2008	>247 793 000	96.13 %	10589 (14098)	7311 (69.0%)	3278 (31.0%)
2009	>261 088 000	99.20 %	11606 (16385)	7422 (63.9%)	4184 (36.1%)
2010	>233 705 126	91.99%	12951 (22172)	7355 (56.8%)	5596 (43.2%)

In Table 1, the column "Active IMO ships" represent the number of specified, active ships (fuel consuming according to the model) for which the use of AIS equipment and registration with the IMO to obtain a unique registry number is mandatory. The amount of these ships between 2006 and 2010 has increased no more than 8%. Comparing the increase of active ships with the increase in annual amount of all

encountered ships reveals that the amount of singular AIS messages and unknown vessels with inconsistent route data has become a frequent issue to deal with. The main reason for this increase in vessels is that smaller ships are installing AIS messaging equipment more often and most likely, sometimes with incorrect settings.

In the recent years, also the amount of active ships without proper IMO number has increased. These vessels have to be modelled without accurate ship specifications. As it was presented in Chapter 3.1, an unidentified ship is assumed to be a small tug boat. The unidentified ship is attributed with a weight of 700 tons and a relatively powerful main engine of 2300 kW, given by average specification of the listed known tug boats. This assumption, however, results often in low engine load estimates. Indeed, recent emissions estimations presented in Chapter 6 have shown a significant increase in CO emissions for tug boats only, which (with the Sarvi's CO emission factor curve) implies very low engine load estimations for the ship type in general.

It should be safe to assume unidentified vessels to be considered to be small ships with an average weight of couple of hundred tons, but the average attributes of these unknown vessels should be re-evaluated. It turns out that active ships without an IMO number are encountered most frequently during summer which suggests that large amount of these vessels are possibly passenger ships. However, it is difficult to obtain any other information about these vessels. One possibility is to use the new sub-program that processes the input data to check for each unknown vessel, for example, how fast it travels, what kind of trips the ship makes and based on this, make more sophisticated guesses about the attributes of the ship. Until more accurate estimates are available, at least the main engine power should be reduced to a level which will not cause these unidentified ships to travel with low engine load estimates.

The total contribution of tug boats and unknown vessels measured in fuel consumption is nevertheless small (10% in 2009) and would most likely be even further reduced after correcting the preset values for unknown vessels. Therefore, if the emission estimation model would be expanded further and used e.g. for computationally heavy dispersion modeling later on, it might be wise to separate these ships from the rest of the input data altogether to reduce the amount of calculations.

4.4.3 AIS coverage correction

The yearly temporal coverage of AIS messages presented in Table 1 varies around 92-99% for the past few years containing several long blackout periods, some with identifiable causes (e.g. severed cable in a construction site in June 2006). Also, blackouts for approximately 24h have not been uncommon, but the source of these blackouts is still being investigated. In any case, AIS shortages are often needed to be taken into account when total emission estimates are produced with the model.

In order to take these temporal AIS blackouts into account, it is needed to understand the interpolation logic of the model. The interpolation logic of the model works as follows: If the distance of subsequent messages A and B is lower than 150km and no more than a day have passed, then STEAM2 model interpolates a travel route for the ship from A to B if and only if the ship with its listed maximum speed could sail from A to B in time. Temporal AIS coverage based correction of emission amount is then rather straightforward a procedure for long blackout durations but gets more complicated if the time interval contains a large amount of short blackouts - During short AIS blackouts, some routes are still being interpolated resulting in a rough, undervalued emission estimates for the time period in question.

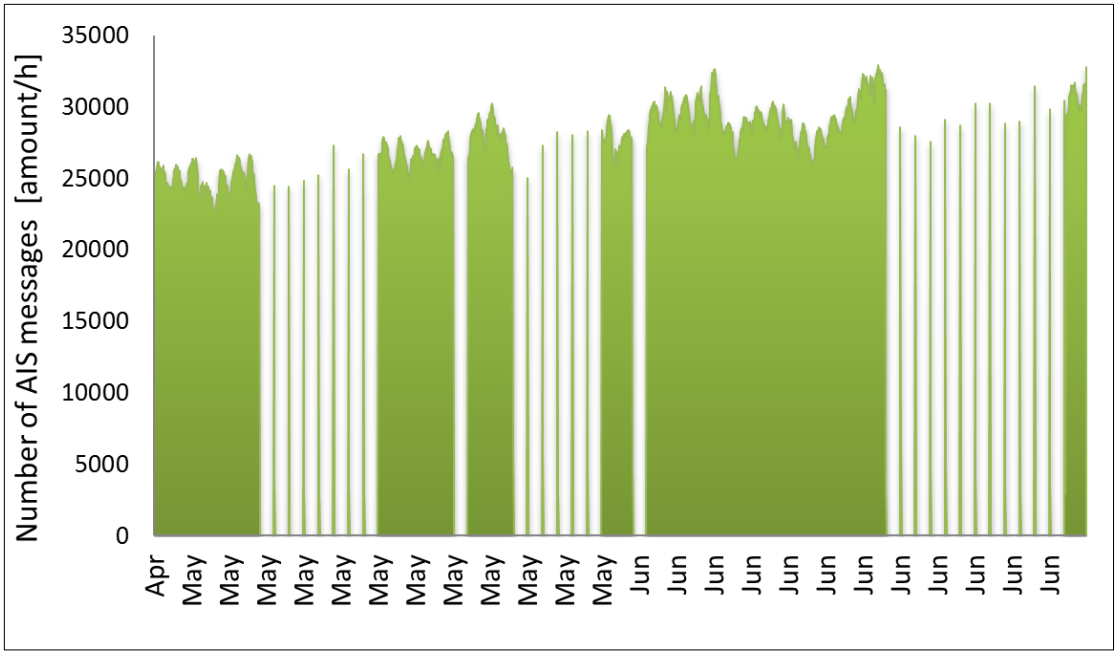

Figure 10: Hourly number of AIS messages received between May and June of 2010. The blacouts presented in the figure are approximately 23h long and are commonly followed by one hour of full coverage during 00:00 – 01:00.

In 2010 short AIS blackouts of 23 hours due to some unknown technical problem with the servers of Helcom were so frequent that the total coverage of several months dropped below 60%. The AIS coverage during the most notable blackouts in 2010 is presented in Figure 10.

To correct the total emission estimates it was needed to solve how much of the ship traffic the model was able to interpolate over the systematic blackout periods. After several test runs it was concluded that $30\% \pm 4\%$ of the daily ship traffic is interpolated by the model for each blackout that lasts approximately one day. In the test procedure, estimated emissions over several time intervals with full AIS coverage were compared against respective time intervals with systematic AIS blackout sequences using the same days of week in comparison. When emission estimates for the year 2010 was finally produced, the importance of taking the interpolation feature into account was over 10% of monthly emissions for some months with very low AIS coverage.

4.5 The revised relation between PM-emissions and SFOC

Engine efficiency is defined as the produced shaft power per energy in the supplied fuel and thus the SFOC value can be viewed as a measure of efficiency of the engine. Engines with higher base SFOC values need to consume more fuel per produced kWh because of the lower efficiency due to engine wear, suboptimal design and combustion timing, etc. Also, the cylinder diameter is affecting the efficiency significantly and therefore small diesel engines have an efficiency of 25% whereas that of very large engines exceeds 50% (Kuiken, 2008). In all situations the combustion process can be assumed complete independent on engine load and SFOC.

In this paper, it has been presented that PM emissions are affected by engine load through SFOC curve meaning essentially that increase in fuel consumption is associated with an increase in PM emissions. The amount of emissions, however, is calculated with fixed emission factors measured in g/kWh even though the amount of fuel combusted in the process could be quite different depending on engine load and between different engines. This raises a question – would it not be more meaningful to measure PM emission coefficients as emissions per fuel burned [g/kg]? Indeed, in some studies in literature, emission factors are presented in grams per fuel burned, but in many cases even these coefficients are derived directly from g/kWh values using a fixed SFOC value. Some studies even seem to deliberately avoid the discussion arising

from problem of variable fuel consumption per power output. This makes it difficult to compare measured emission coefficients if the used engine's fuel consumption is not specified.

The conservation of matter –principle suggests that the sulphur content of the fuel has to be converted to either sulphur oxides or to sulphate and the amount of these compounds must be directly linked to the amount of fuel burned. If not, then sulphur would start cumulating inside the engine. Also, major source of ash particles in the exhaust gas originate from the ash content of the fuel and thus ash particles in principle should correlate strongly with fuel consumption as well. However, the formation reactions concerning the other particles of PM such as OC and EC might not be bounded by such principles.

Currently the base SFOC value is not affecting estimation of PM even though it is primary factor affecting the fuel consumption; in the internal ship database there are base SFOC values that range from 160g/kWh to 230g/kWh.

4.5.1 Emissions coefficients based on emissions per consumed fuel

To overcome the inconsistencies with emissions and their relation to fuel consumption mentioned above, a new base SFOC dependent emission factor for PM was formulated which also affects to the estimated amount of SO_X emissions as well. It should be noted that the suggested changes are only to make the principles of PM emission estimation more consistent. More measurement data for the suggested modifications are needed to check if the changes would actually result in more accurate estimations.

While the new suggested formulation for the PM emission factor produces consistent emission amounts with the amount of fuel burned. However, the new solution involves a problem – the current emission factors provided by IMO GHG2 are based on measurements from Germanischer Lloyd's institute but unfortunately, no engine specifications are available concerning that particular study besides the fact that the test was performed with a 2-stroke type engine. Thus the current emission factors that are used in the model cannot be associated with a specific base SFOC. Given the base SFOC value, however, the total PM emission factor of the model could be expressed in following manner:

$$EF'_{PM} = SFOC_{base}(0.455EL^2 - 0.71EL + 1.28)(a + bS) \quad (35)$$

where coefficients a and b can be determined given the IMO GHG2 engine specifications or with a new similar emission factor study measurements with provided engine specifications. Another equivalent yet simpler way of expressing the new PM emission factor is in the following form

$$EF'_{PM} = \frac{SFOC_{base}}{SFOC_{baseGL}} * EF_{PM} \quad (36)$$

where $SFOC_{baseGHG2}$ is the currently unknown base SFOC value for the engine that was used in determining EF_{PM} in Chapter 3.5.2. For now, let's roughly assume that the current emission factors were determined using a typical large 2-stroke engine with a fuel consumption of 170g/kWh. The resulting new PM emission factors with several different base SFOC values are presented in Table 2.

Table 2: The new PM emission factors as a function of base SFOC and fuel sulphur content (S, in units of mass percentages).

Base SFOC Factors [g/kWh]	170g/kWh	190g/kWh	210g/kWh	230kWh
EC	0.05	0.056	0.062	0.068
OC	0.2	0.224	0.247	0.271
Ash	0.05	0.056	0.062	0.068
SO_4	0.312	0.349	0.385	0.422
H_2O $assoc.$	0.244	0.273	0.301	0.330
$Total\ PM$	0.3 + 0.556S	0.34 + 0.62S	0.37 + 0.69S	0.41 + 0.75S

As Eq. 36 suggests, only if the base consumption of fuel is equal to the engine of Germanischer Lloyd study, then the fuel consumption based PM factor is the same as before. Furthermore, in Chapter 3.3 it was presented that in the model the base SFOC depends on the age, stroke type and size of the engine in a manner that was suggested in (Buhaug, 2009). Thus, the refined way of determining the PM emission coefficients would indirectly cause these factors to affect PM emissions through base SFOC as they already do with SO_X and CO_2. For example, the base SFOC for a four stroke main engine of 1000kW made in 1980 would be estimated to be 230g/kWh. The resulting PM emission factors would then be in fact 35% greater than the model currently estimates.

As it was shown previously that currently a large portion of the total active vessels are not specified in the ship database and thus are assumed to be small vessels equipped with engines similar to the one in the example. Therefore, the suggested new PM emission factor would most likely increase the estimated PM emission amounts notably. Indeed, in a preliminary test using AIS data from May 2010, two emission simulations (with and without the new PM emission factor) were compared. The test showed that the PM estimates might be approximately 15% more than the model currently suggests.

4.5.2 SO_x emissions using the new PM emission coefficients

In Chapter 3.5 it was shown that the amount of SO_X is calculated subtracting the sulphur mass of SO_4 from the sulphur mass of the burned fuel. PM emissions are not completely in terms with the amount of fuel burned as it has been discussed in this chapter but SO_X however is. This has led to a variable ratio between the emission amounts of SO_X and SO_4. Indeed, it can be seen in the annual emission estimates presented in Chapter 6 in which the ratio of SO_X and SO_4 is slightly different for every year implicating that the ratio of SO_X and SO_4 emissions is dependent on the base SFOC of the individual ships without intended physical reason.

The amount of SO_X emissions can be calculated in a more consistent way: the conservation of mass principle dictates that for any amount of fuel burned the amount of sulphur in SO_X and SO_4 emissions must be equal to the amount of sulphur in the burned fuel and thus, for any given fuel amount the SO_4 emissions can be calculated using the new PM emission factor from Table 2. Using these new, more fuel consumption dependent emission factors, it can be calculated that the ratio between the two emission masses (m_{SO_X}/m_{SO_4}) discussed in Chapter 3.5 would be reduced to 11.5 (and even less than 11.5 if the base SFOC of the Germanischer Lloyd study was actually lower than 170g/kWh). Hence the conversion ratio of sulphur to sulphate would now be slightly larger than it is currently in the model but this time, unaffected by base SFOC as intended.

To make matters even more complicated, in a recent study by Petzold it was presented that for several test engines the sulphate conversion ratio followed a linear, increasing trend as a function of engine load (Petzold, 2009). In the study, sulfate emissions increased by a factor of 3 when engine load was raised from low load (20-25%) to high

load (75-85%). However, the conversion rates were observed to be lower than in the model with all engine load points. Thus it is possible that sulphate emissions and therefore also PM emissions are even more dependent on engine load and are being overestimated especially in the lower engine load states. Hopefully, more measurement data of PM emissions with different load points is available in the future and the effect of engine load to sulphate conversion can be verified and taken into account if necessary.

4.6 NO_x emission modelling using combustion time

The purpose of the proposed modification presented in Chapter 4.3 was to harmonize the assumption how the engine load and fuel consumption together affects PM emissions. In contrast to PM emissions, it was stated in Chapter 2, that NO_X emissions are not affected by engine load nor fuel consumption, but depend rather on the engine's rated RPM. Based on the latter, it is natural to assume that the instantaneous NO_X emissions depend on the current RPM of the engine. However, the current RPM is actually a function of the engine load, which implies that NO_X emissions are indeed affected by engine load. It would seem that the assumptions of NO_X formation reactions need to be harmonized as well, and hence the nitrogen reactions with oxygen are studied here with greater depth.

In typical marine diesel engine combustion, approximately 170g of fuel, 1,3g of lube oil and 7.8 kg of air is used per each produced kWh. 78% of air is nitrogen and 21% is oxygen. The exhaust gas usually contains approximately 0.5 kg of CO_2, 0.2kg of vaporized water and also 1.1kg of excess oxygen (Kuiken, 2008). Nitrogen reaction requires time, oxygen and a high temperature. Clearly, the abundant oxygen cannot be the bottleneck for nitrogen reactions and thus there are left only two factors to account for – time and temperature.

4.6.1 Reaction time for NO_x formation

According to Sarvi, for any given two engine states (EL,RPM) the relation of engine load and speed for a typical marine diesel engine is as follows:

$$\left(\frac{RPM}{RPM_2}\right)^2 \sim \left(\frac{EL}{EL_2}\right) \tag{37}$$

Substituting RPM_2 with the maximum rated RPM and fixing EL_2 then with the value of 1, the RPM of the engine as a function of engine load is given by

$$RPM = a * RPM_{MAX}\sqrt{EL} + RPM_{MIN} \tag{38}$$

where a and RPM_{MIN} are engine specific constants, which determine the minimum engine speed that is needed for the engine to run on low engine loads. For Eq. 38 to give meaningful values, the following must apply for full engine load with maximum RPM:

$$RPM_{MAX} = a * RPM_{MAX} + RPM_{MIN} \tag{39}$$
$$=> a = (RPM_{MAX} - RPM_{MIN})/RPM_{MAX}$$

For the test engine used by Sarvi, the coefficients can be derived with linear regression: a = 0.74 and RPM_{MIN} = 133.6. Indeed, the engine load in the Sarvi's study seem to drop to below 0.25 with speeds lower than 60%% of the rated RPM. Studies made by Agrawal shows that Eq. 38 used with these coefficients agrees with at least 3 other engines of different sizes.

In a 2-stroke engine, the total combustion cycle is done once for each revolution of the crankshaft whereas the 4-stroke engines use two revolutions for the total cycle. The total combustion process including expansion takes approximately 120 crank degrees and with 4-stroke engine about 140 degrees according to Kuiken (Kuiken, 2008). Thus, the reaction time for nitrogen reaction is given by:

$$t = \frac{60}{RPM} C_{str} \tag{40}$$

where C_{str} is $140°/720°$ for 4-stroke and $120°/360°$ for 2-stroke. Using Eq. 38 and 40, the reaction time can be calculated for any engine with a specified speed rating. Currently, the rated RPM value of the main engine is not specified for only 3.73% of the ships in database.

The number of revolutions per minute varies significantly; from 100 up to 2000 revolutions and thus the reaction time for NO_X formation varies even more between engines as the fastest engines are usually 4-stroke engines with a smaller value of C_{str}. In Figure 11, measured NO_X emission factors from four separate studies (Agrawal 2008,

2009, 2010), (Sarvi, 2008) are presented in function of calculated reaction time given by Eq. 40.

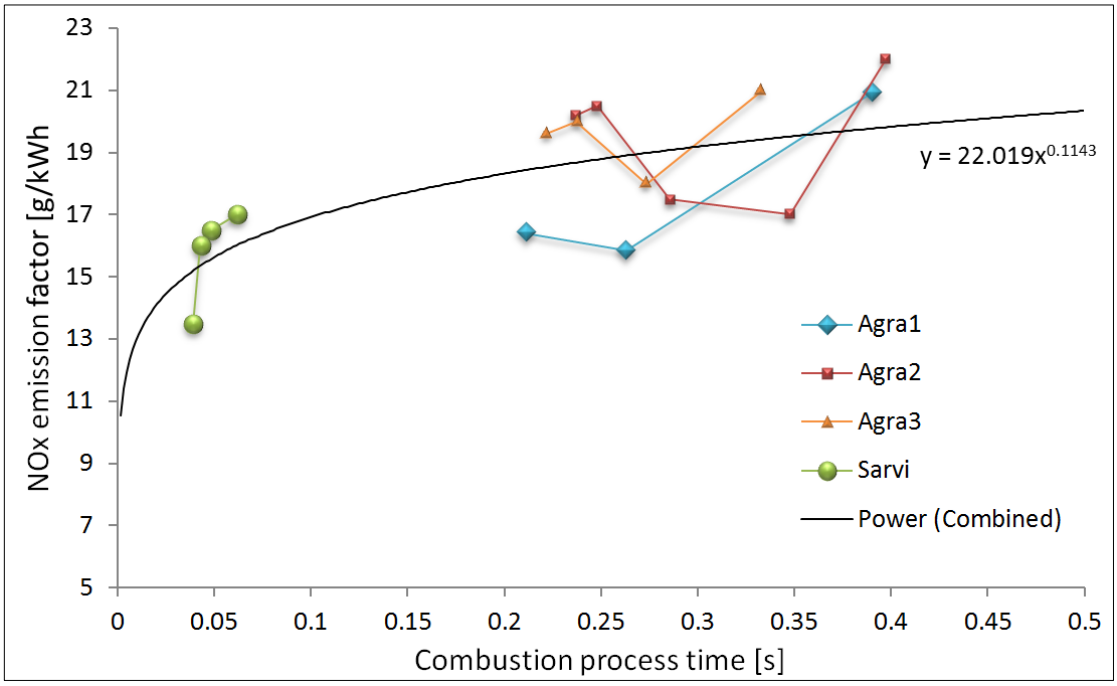

Figure 11: Measured NO_X emission factors plotted against calculated reaction time. Measurements are from 4 separate studies conducted by Agrawal (3 studies) and Sarvi (one study). Also a regression power series (black line) for the combined measurements are presented. All the engines are Tier I type.

The correlation for the regression line is just above 0.5. Indeed, a linear regression line would do just as well for the data presented in Figure 11 but in general the NO_X emissions from high speed engines are proven to have a significantly lower emission factor and therefore the regression line should decrease rapidly as reaction time approaches zero. Unfortunately, there are currently no applicable emission measurements available for high speed engines.

4.6.2 Temperature in NO_x formation process

By looking at the variation of the NO_X emission coefficients in Figure 11, it is apparent that reaction time alone isn't sufficient for accurate estimates. Kuiken suggests that the role of ambient temperature in the reaction is so profound, that the amount of formed NO_X particles per second approximately ten-folds if the temperature is increased by 100 degrees. This suggestion is backed up by measurements by Sarvi, who presented that the peak temperature would be the main factor for NO_X emissions. On the other hand,

it was also suggested by Sarvi that the speed of the engine affects the temperature as well.

Clearly, the engine load is affecting the amount of NO_X emissions, but most likely through reaction time and combustion temperature and thus the NO_X modeling is currently reasonable to be based on the IMO tier I curve alone. If more NO_X emission factor measurements are made available, especially ones that are conducted with high speed 4-stroke engines then a more reliable model for NO_X emissions could be implemented based on the idea of reaction time. The effect of this implementation would most likely result in a notable increase in the amount estimated NO_X emissions (10-20%) near harbor areas, where ships tend to sail with low engine load. It is likely that the combustion temperature of the engine is not something the model can or should be able to do and thus should be left out of the NO_X emission modeling.

4.7 Alternative marine fuel – Liquid Natural Gas (LNG)

IMO and EU both seek to decrease emissions arising from marine traffic by enforcing legislations and directives, for example, by setting a maximum limit for the amount of sulphur in marine fuel-oil. Other example is the IMO tier III (presented in Figure 4) curve that defines the maximum NO_X emission factor for engines installed after January 2016. Currently, there are a few main options to achieve such a drastic reduction of approximately 80% in NO_X emissions – some involve the use of various abatement methods presented in Chapter 2 and some include the usage of alternative fuels, such as liquid natural gas, LNG.

The use of LNG fuel practically eliminates all of the PM emissions and due to lower burning temperatures, also NO_X emissions are reduced significantly. LNG fuel does not contain any sulfur and thus, all of the SO_X emissions are eliminated. In addition, using LNG incorporates no risk of environmental or safety hazards (excluding from high pressure) as it needs very specific temperature and pressure -conditions in order to be volatile in its gaseous form. However, LNG must be maintained cold to remain a liquid and to fulfill that requirement the LNG is to be stored at about 100°K as a boiling cryogen, which inevitably reduces the efficiency of the overall solution. Also, the LNG vapor boil off produced during changes of state must be let out to allow the storage temperature to remain constant (Zbaraza, 2004). Because of this, LNG is becoming

increasingly popular among LNG tankers themselves, as it is possible to salvage large amount of boil off vapor for propelling power.

4.7.1 Emission modeling with ships using LNG fuel

In Table 3, a comparison of emission factors between LNG and diesel according to Wärtsilä is presented. The NO_X emissions are reduced approximately 85% per kWh and also CO_2 emissions are measured to be significantly lower. According to (Zbaraza, 2004) PM emissions are reduced approximately 70% and in a recent report from DNV it was suggested that the PM reduction is almost 100% (DNV, 2011).

Table 3: CO_2 and NO_X emissions from a duel fuel engine according to Wärtsilä. For both operation modes (diesel and gas) measurements were made using two different load points.

	Diesel		LNG	
Engine Load	**0.75**	**1**	**0.75**	**1**
NO_X	22g/kWh	11.5g/kWh	2g/kWh	1.4g/kWh
CO_2	630g/kWh	630g/kWh	450g/kWh	430g/kWh

Typical LNG fuel consists mostly of methane (92-99.7%) and ethane (0.1 – 9.3%) and therefore approximately 75% of the mass in LNG fuel is carbon. Therefore, in perfect combustion process, in which every carbon atom is assumed to be oxidized, one gram of LNG fuel produces approximately 2.76 grams of CO_2. Diesel fuel, on the other hand, contains more carbon by mass (approx. 85%) and produces 3.04 grams of CO_2 per burned fuel gram. Also, LNG has a higher heat value than diesel – Comparing the lower heat values (LHV) reveals that LNG combustion produces 14% more heat. Using the higher heat values (HHV) that takes into account also the residual heat in the exhaust gas, the difference between the two fuels is even more distinctive: 18% more heat from LNG if all of the residual heat from exhaust gas gets successfully utilized from using both of the fuels.

Currently, most of the marine engines that are capable of using LNG fuel are so-called dual-fuel engines and are designed to use small amounts of marine diesel oil, especially with low engine loads. Measurements made by Wärtsilä suggests that the shape of a SFOC curve for dual fuel LNG engine is similar to diesel engines, although the fuel consumption increases more steeply in the lower engine load reaching up to 175% with

very low engine loads (Zbaraza, 2004). Indeed, because of this, current dual fuel engines prefer to run fully on diesel if engine load drops below 40%, which would make emission modeling more complicated. The overall efficiency of the dual fuel engine is also more than 20% lower when compared to diesel engine, but the efficiency ratio is likely to increase and ultimately challenge diesel engines after the relatively new LNG technology has been adopted properly.

Assuming the lower efficiency of the current LNG engine technology (-23%), the relative CO_2 emissions reduction potential of LNG compared to diesel can be calculated to be:

$$Reduction\ potential = 100\%\left(1 - \frac{1.23 m_{CO2LNG}}{m_{CO2Diesel}}\, r_{HV}\ \right) = \tag{42}$$

$$100\%\left(1 - \frac{1.23 * 2.76g * 42612Jg^{-1}}{3.04g * 48632Jg^{-1}}\ \right) = 7.3\%$$

where m_{CO2LNG} is the amount of CO_2 produced by burning one gram of LNG, $m_{CO2Diesel}$ is the respective amount by burning marine diesel oil and r_{HV} is the ratio of heat values of the fuels. Thus, using LNG for marine vessels might result in 7.3% reductions for CO_2 as a worst case scenario. Let's assume the same overall efficiency for using both fuels. Then the relative reduction is equal to

$$100\%\left(1 - \frac{2.76g * 42612kJg^{-1}}{3.04g * 48632kJg^{-1}}\right) = 22.3\% \tag{43}$$

Using the higher heat values i.e. assuming that all of the residual heat can be captured from the exhaust gas, the theoretical upper limit for CO_2 reductions can be calculated to be

$$100\%\left(1 - \frac{45575kJg^{-1}}{55206kJg^{-1}} * \frac{2.76g}{3.04g}\right) = 26.8\% \tag{44}$$

Depending on calculation method and efficiency of the LNG engine, the reduction potential for CO_2 varies from 7.3% to a maximum of 26.8%. Because all of these presented beneficial aspects in using LNG fuel in marine vessels, policy makers are currently very interested in getting their hands on scenario analysis about partial and full adoption of LNG technology. Therefore, LNG as a marine fuel has been added to the

emission model STEAM2 using a rough average reduction of 20% for CO_2 assuming complete reduction in PM emissions. If LNG technology increases its popularity, then it might be worthwhile to model the use of LNG fuel in a more sophisticated manner, which might involve applying a steeper SFOC curve for LNG fuel and also taking into account the dual-fuel engine's diesel fuel usage with lower engine loads.

4.8 Route interpolation with a shortest path algorithm

As a result of AIS blackouts, sometimes the travel route interpolation has to be done over long distances using a straightforward line connecting the two locations. Inevitably, these lines often go across continents and islands. Because of this, also the estimated speed for this route is significantly underestimated when a constant speed estimate for the line route is calculated. The other simple option, to use the last known speed data for the route, might naturally result in even larger margin of error. Sometimes the cause of this problem is not just temporary as it is with AIS shortages – there are significant geographical gaps in AIS coverage as well. Indeed, if STEAM2 emission model would be used in the Mediterranean Sea or the North Sea, a more sophisticated route interpolation feature would be most welcome.

To resolve the interpolation problem, a shortest path algorithm can be used to calculate the most probable and plausible marine route connecting any two end points in any sea region. To save computational time, however, this alternative interpolation method is to be used only if the result from straight line interpolation would be evaluated unsuitable, for example, in case the line interpolation would suggest a route through land.

The main idea of the algorithm is to use a node grid that defines the sea surface – A node has a value of 0 if it is on land and otherwise has a value of 1 indicating a marine region. To generate the node grid, a Matlab function was produced, which evaluates a RGB (red, green, blue) value for each pixel in a selected map-picture. In the picture, any sea surface has been distinctively colored, for example, in pure red. The resulting binary node grid is then repeatedly used by the model to check weather a node or a coordinate is on the sea surface or not.

The problem of finding the shortest path is also solved using the same node grid. The shortest path algorithm itself is beyond the scope of this thesis and the related shortest path network optimization problem is discussed in greater detail in (Johansson, 2011). In short, the problem is formulated as follows: There exists and outbound arc from any

marine node to each adjacent marine node (maximum of 8 out bound arcs including 4 diagonal arcs). Each arc is associated with a cost of traveling through it, and the cost of doing so is set to be equal to the Euclidean distance between the two nodes. The shortest path is generated using a Djikstra label setting shortest path algorithm which initially associates infinite costs of travelling from the source node (s) to any other node marking the current travel costs with labels. Then the problem is reduced into finding routes with smaller total costs to each node, and in case a better route has been identified the current label is rewritten to match the cost of the better route. The process is repeated until the labeled cost to the target node can no longer be made smaller.

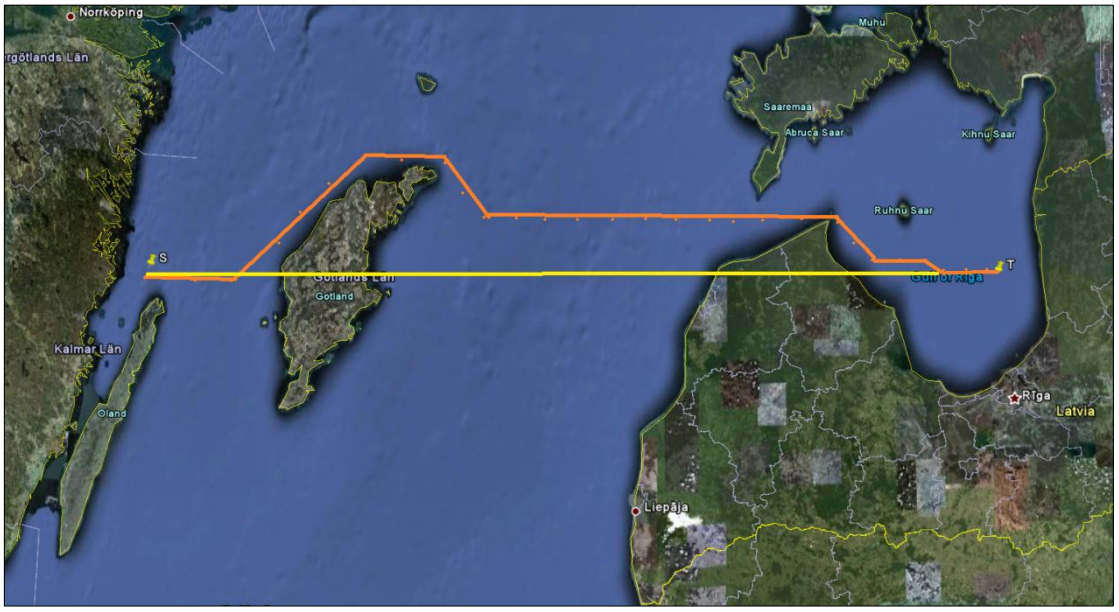

Figure 12: Shortest path example from s to t using a 100x100 node grid. The solved shortest path is presented with an orange line and the route interpolated with the regular method is presented as a yellow line. Map is provided by Google Earth.

In Figure 12, an example route produced by the algorithm is presented. In this example, a ship's last message before an unknown blackout occurred was sent in the place marked as s (source) near Vaestervik of Sweden. After 20 hours later the ship continues sending AIS messages from t (sink) in the Gulf of Riga. Using the two endpoints the model is able to calculate the shortest and thus a probable route from s to t without traveling through land. The final cost label for the node t given by the algorithm indicated that the minimum travel distance is 472 kilometers and therefore the ship is assumed to travel the distance with a constant speed of 6.6 m/s. The traditional interpolation method using a straight line connecting s and t leads to a travel

distance of 7 degrees in longitude, which translates to 420 km (57.5° in latitude) with a constant speed of 5.8 m/s respectively.

In this example, a very rough node grid of 10 000 nodes covering the whole Baltic Sea was used. Due to the scarcity of the grid, the resulting shortest path (orange line) problem was solved in a fraction of a second. In contrast, solving the problem using a more detailed grid map of 500x500 nodes would take more than a minute using a modern PC but would produce smoother routes with better resolution. Indeed, it is crucial to use the more intelligent interpolation feature only when it is needed. For instance, the method could be used only if

- The vessel in question has a substantial impact on emissions
- The distance between s and t is large enough
- A normal interpolation method would result in route that travels through land

Using the presented criteria it is possible to increase the resolution of the method if needed without causing unnecessary increase in total computation time. The first criterion could be determined by checking if the vessel has a valid IMO number or not. A proper cut-off distance for the second criterion could be set to equal 10-50 km. The third clause has been already programmed to the algorithm using the logical node map by checking all the non-marine nodes, if any, in between s and t. Finally, the computational effort required by the algorithm can be significantly reduced by using a set of different maps with different resolution and geographical scope.

5. Model evaluation

In this chapter, the extended model is evaluated against available experimental data. Selected numerical results, including the comparison of annual fuel statistics and model estimates are presented.

5.1 Evaluation of the predictions of STEAM2 for engine power

An example comparison between the predictions on main engine power of the two model versions is presented in Figure 13. The engine power data has been measured in this study at the engine room of a large RoPax (Roll On – Roll Off cargo/Passenger) vessel. The presented voyage was done in an archipelago area near Stockholm, Sweden, and in the vicinity of this archipelago, in April 2008. This specific dataset is used, as it was the only one available in the Baltic Sea region. Measured power profiles, such as the one presented in Figure 13, are difficult to obtain, as only a limited number of vessels have internal equipment suitable to collect this data.

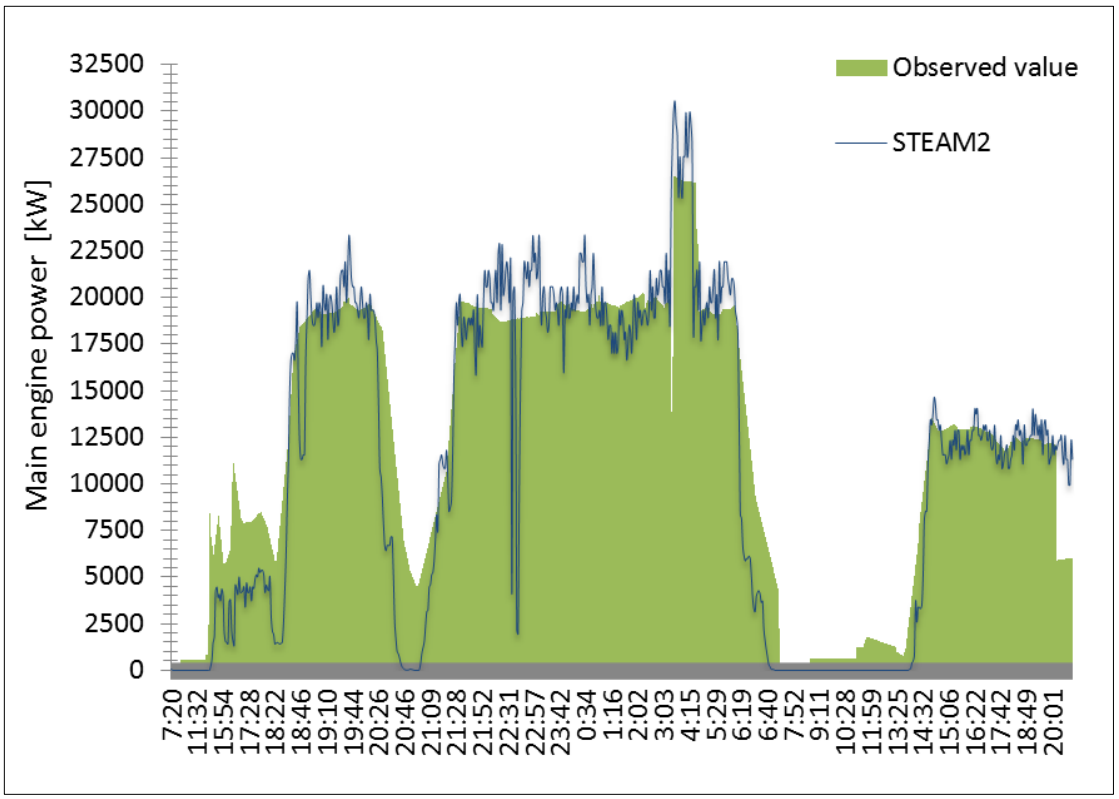

Figure 13: The predictions of the STEAM2 model and the corresponding measured engine power. The data has been measured for a 60 000 t RoPax vessel that was sailing in the Baltic Sea within and near the archipelago surrounding the city of Stockholm in April 2008.

The basic statistical measures of this comparison are presented in Table 4. The predicted main engine power of model is in a fairly good agreement with the measured values. The predictions of the STEAM2 model are moderately better that those of previous model version in terms of the mean absolute error, and vice versa in terms of the mean error. STEAM2 slightly under estimated the engine power. There are physical factors that have been neglected in both models, such as the influences of the sea ice on the kinetic energy of the ship, the squat effect and the sea currents. The model would therefore be expected to under-predict the required engine power.

Table 4: Statistical measures for the power predictions of STEAM2 model. P is the predicted power, P_M is the measured power and the number of observations n = 729. Errors in percent in the table have been computed with respect to the mean values of the measurements.

	Formula	STEAM2	Measured (M)
Mean value	$\frac{1}{n}\sum P$	11190kW	12338kW
Mean Error	$\frac{1}{n}\sum (P - P_M)$	-1148kW (-9.3%)	-
Mean Absolute Error	$\frac{1}{n}\sum (\lvert P - P_M \rvert)$	1845kW (15%)	-

The Hollenbach method used in STEAM2 results in a steeper power curve compared with the corresponding method in the previous model, i.e., a relatively lower resistance for low ship speeds and a higher one for high speeds.

As it was discussed in Chapter 4.4, the rapid changes in the unprocessed speed data causes problems in estimating current power consumption. Indeed, as it can be seen form Figure 13 the measured power is smooth whereas predicted power is not because of the rapidly changing speed data. The difficulty of modeling instantaneous power and especially changes in engine load arises from the initial problem of estimating engine power based on speed data itself – changes in speed are interpreted as a result of changes engine load but the reality is likely quite the opposite: engine load is usually kept steady for economic reasons and the forces acting on the ship causes the speed to fluctuate. Based on this study, smoothing the speed data by taking the average of the two end point values should be an improvement in itself.

5.2 Evaluation of STEAM2 predictions for fuel consumption

The reported and predicted fuel consumption of a RoPax ship in 2007 has been presented in Figure 14a-b. The extended model predicts the total fuel consumption fairly accurately and slightly over-predicts the fuel consumption of auxiliary engines and boilers, which is a significant improved as the older model version substantially over-predicted (by more than 150%) the latter consumption.

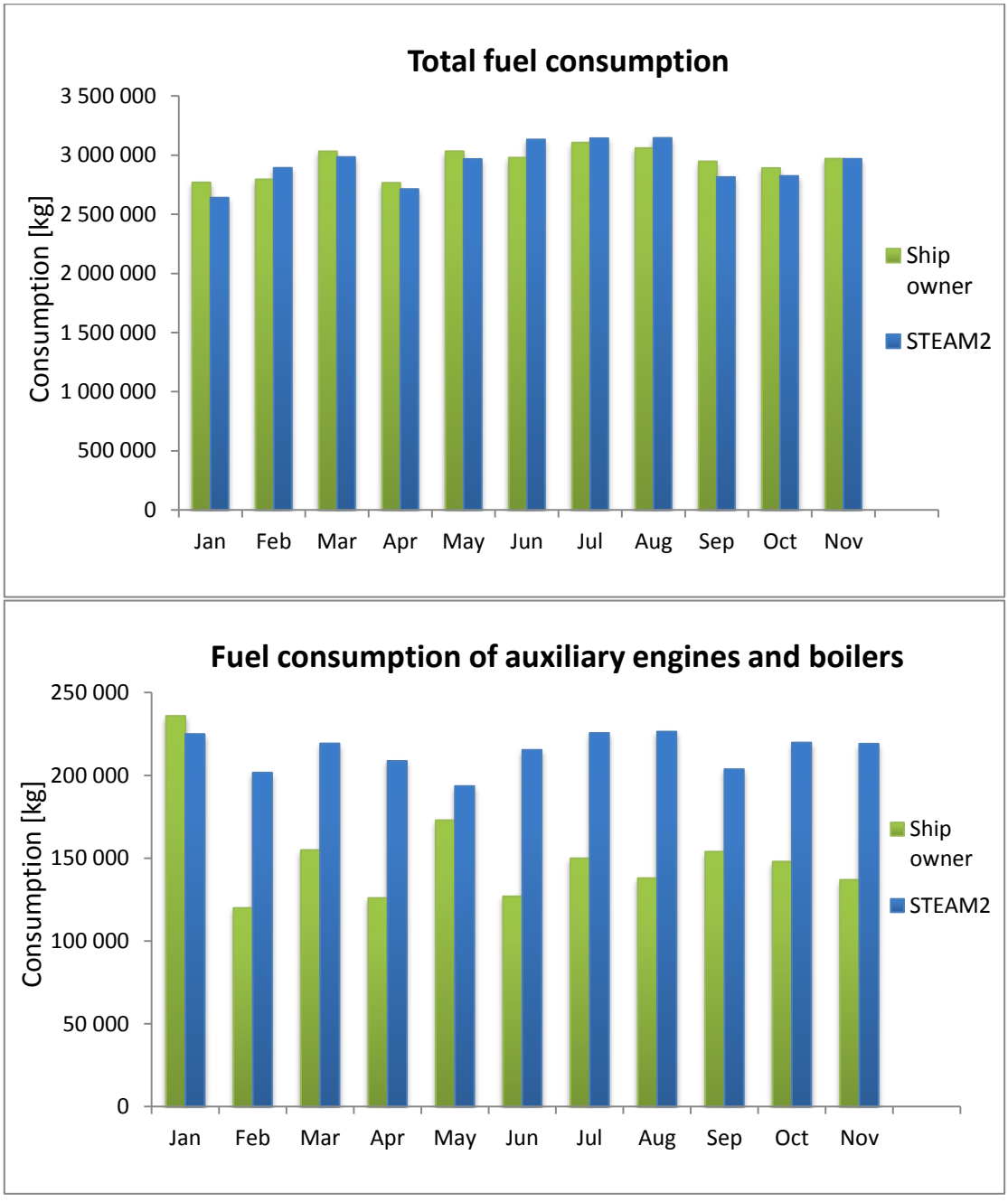

Figure 14a-b: The monthly average fuel consumption of a RoPax ship in 2007, as reported by the ship owner, and predicted by the two model versions. The total fuel consumption is presented in the upper panel, and the fuel consumption of auxiliary engines and boilers in the lower panel.

Similar studies were made with four other RoPax-ships. The results are presented in Figure 15. The overall accuracy of the aggregated predictions is satisfactory. As it was discussed in Chapter 4, the effect of currents would likely reduce the fuel estimates. The addition of kinetic energy, would suggest an increase of approximately 4% and the effect of ice during winter would increase estimates as well.

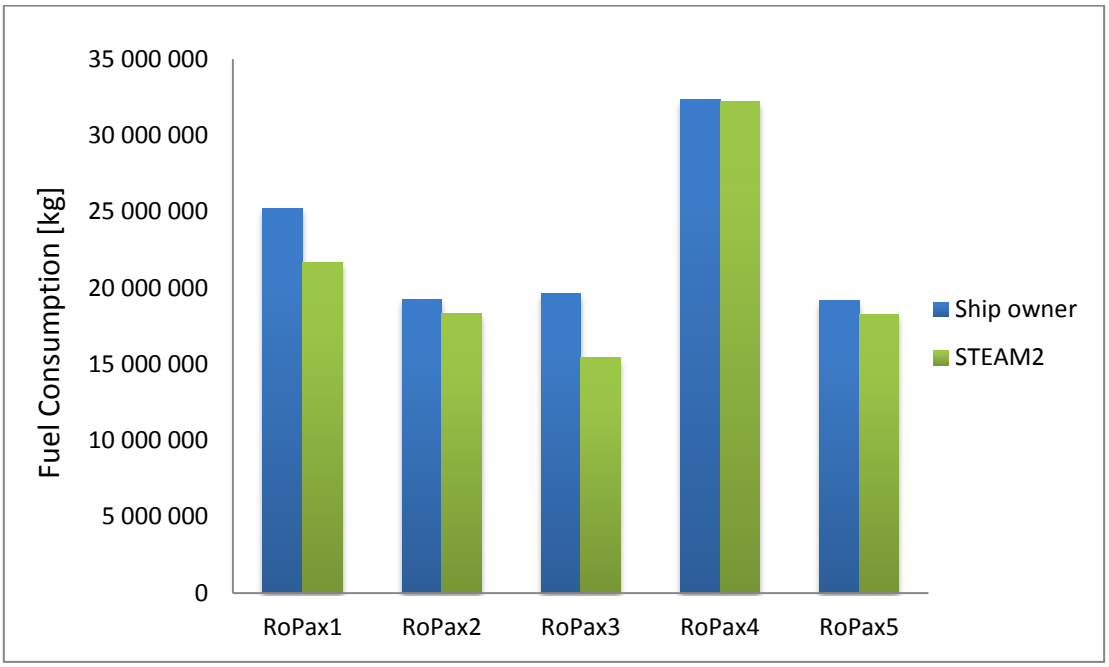

Figure 15: The reported and predicted total fuel consumption for five RoPax vessels from January to November in 2007. The vessel RoPax 4 is the same ship, the data of which has been presented in Figures 7a-b.

5.3 Evaluation of the modeling of load balancing in STEAM2

The model determines the number of engines, which need to be operated to overcome the predicted resistance of the ship, and the engine load of all running engines. The validity of this feature was tested using the measurement data from the cruise presented in Figure 16a-d, in which there were four identical main engines in the vessel considered. The overall accuracy of predicted engine loads is fairly good or good for most of the time in the cases presented. However, there is some inaccuracy in the initial stages of the voyage, and for the fourth predicted engine (i.e., the one used only for very limited time periods). The spikes in the fourth engine's estimated power output suggests that the total power requirement was on the threshold for start-up of engine 4 on several occasions according to the model. In reality, of course, large diesel engines cannot be shut down and start-up in such a frequent manner. In a recent study (Winnes, H., Fridell, E., 2010) it was observed that the startup-of marine engines increases the

amount of emissions significantly for a short duration. If such a feature would be included in the model later on, then it might not be meaningful to use the feature with multi engine setups.

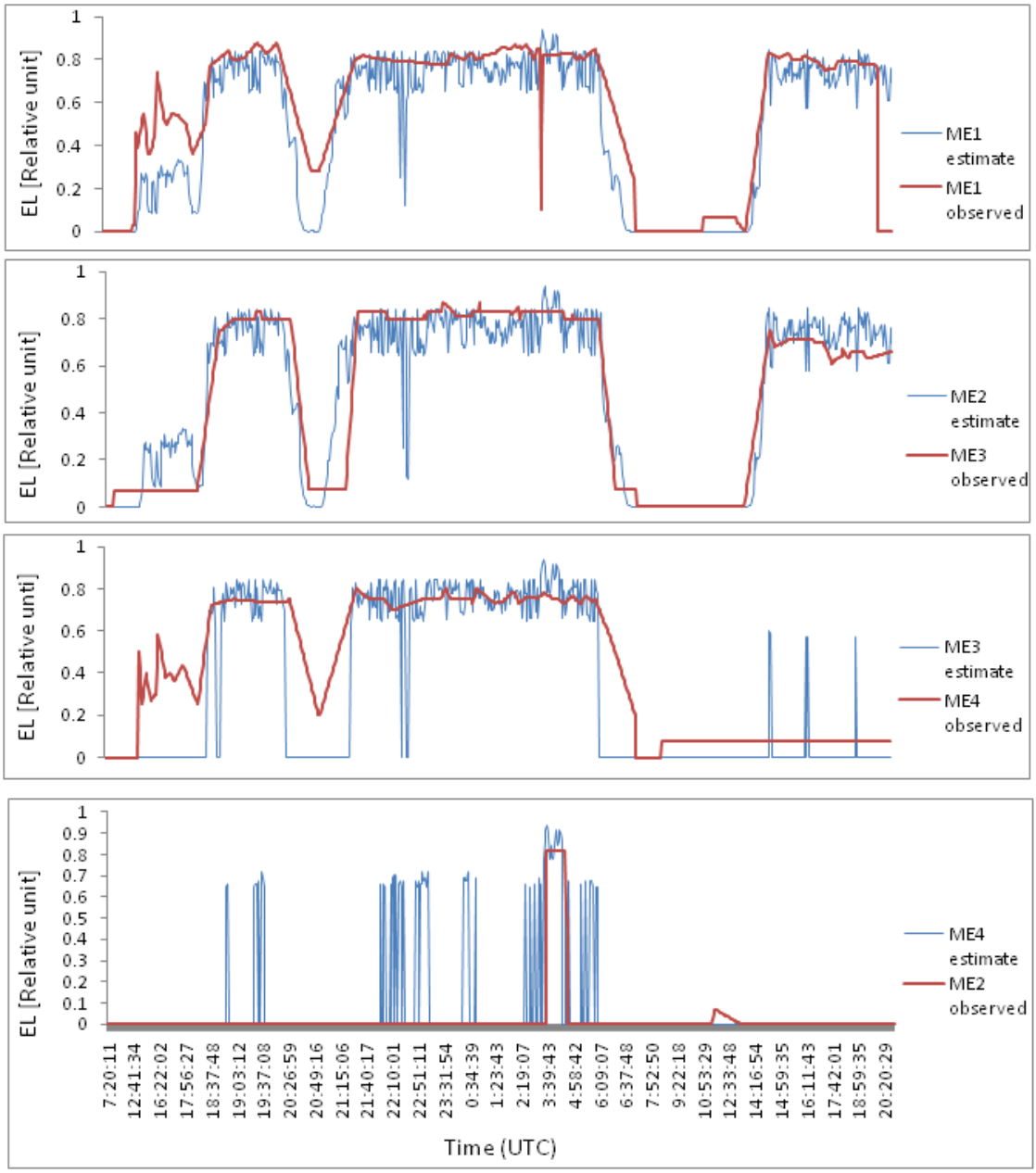

Figure 16a-d: Predicted and observed engine loads of four identical main engines in a large RoPax ship. The time scale for all plots a-d is the same, presented in panel (d). MEx, x =1,2,3,4, are the four main engines. 'Estimate' refers to the prediction of STEAM2. The numbering of the main engines in the model has no influence on the engine load predictions; for instance, in panel (b) the curves ME2 (estimate) and ME3 (observed) are directly comparable.

5.4 Evaluation of the PM emission factors

The emission factor predictions by STEAM2 are compared with measurements available from literature in Figure 17a-d. The engines loads and fuel sulphur contents in these studies are as follows: 85 % and 2.85 % (Agrawal et al., 2008), 84 % and 1.90 % (Moldanova et al., 2009), 85 % and 2.21 % (Petzold et al., 2008), and 57 % and 3.01 % (Murphy et al., 2009). For simplicity, these studies are in the following referred to as AGR, MOL, PET and MUR. The engine load is within the commonly used operation range for the three first-mentioned studies, but it was substantially lower in Murphy et al. (2009). The sulphur content of fuels varies from 1.9 to 3.0 %.

For a substantial fraction of these predictions, STEAM2 is in agreement with the measurements; the agreement is best in case of AGR. However, there are also significant differences. The most significant differences are found in comparison with the data by MOL, especially for OC and SO_4. The predicted sulphate emission factor is approximately three times larger than the measured value. According to MOL, the measured low sulphur conversion to sulphate may be a result of the relatively smaller amounts of V and Ni in the fuel, compared with, e.g., AGR. The catalytic properties of Ni and V enhance the sulphur conversion to sulphate.

According to Petzold et al. (2010), the conversion efficiency of fuel sulphur to particulate sulphate is linearly increasing with increasing engine load from 1 to 5 % (such a dependency is not allowed for in STEAM2). This could be one of the reasons for the deviations of predictions and data in case of MUR, due to the low engine load. A detailed investigation of the complete data set of Petzold et al. (2010) using STEAM2 reveals an increasing difference in S to particulate SO_4 conversion with decreasing engine loads.

In case of MUR and AGR, the ash emission factor was computed from the ash content of the fuel, whereas MOL and PET report directly measured values of ash. These ash emission factors are therefore not directly comparable with each other, and the MUR and AGR ash emission values are strictly speaking not comparable with the STEAM2 predictions. There may be processes during fuel combustion, which lead to changes in the amount of emitted ash. MOL reports the highest ash emissions, although the ash content of the fuel used by MOL is the lowest. In comparison with PET, the STEAM2 ash emission factors are in a good agreement. The ash emissions in principle depend

on the ash content of the fuel, but this is not taken into account in the model. However, one cannot conclude based on the above comparison of predictions and data that this would be a significant impact.

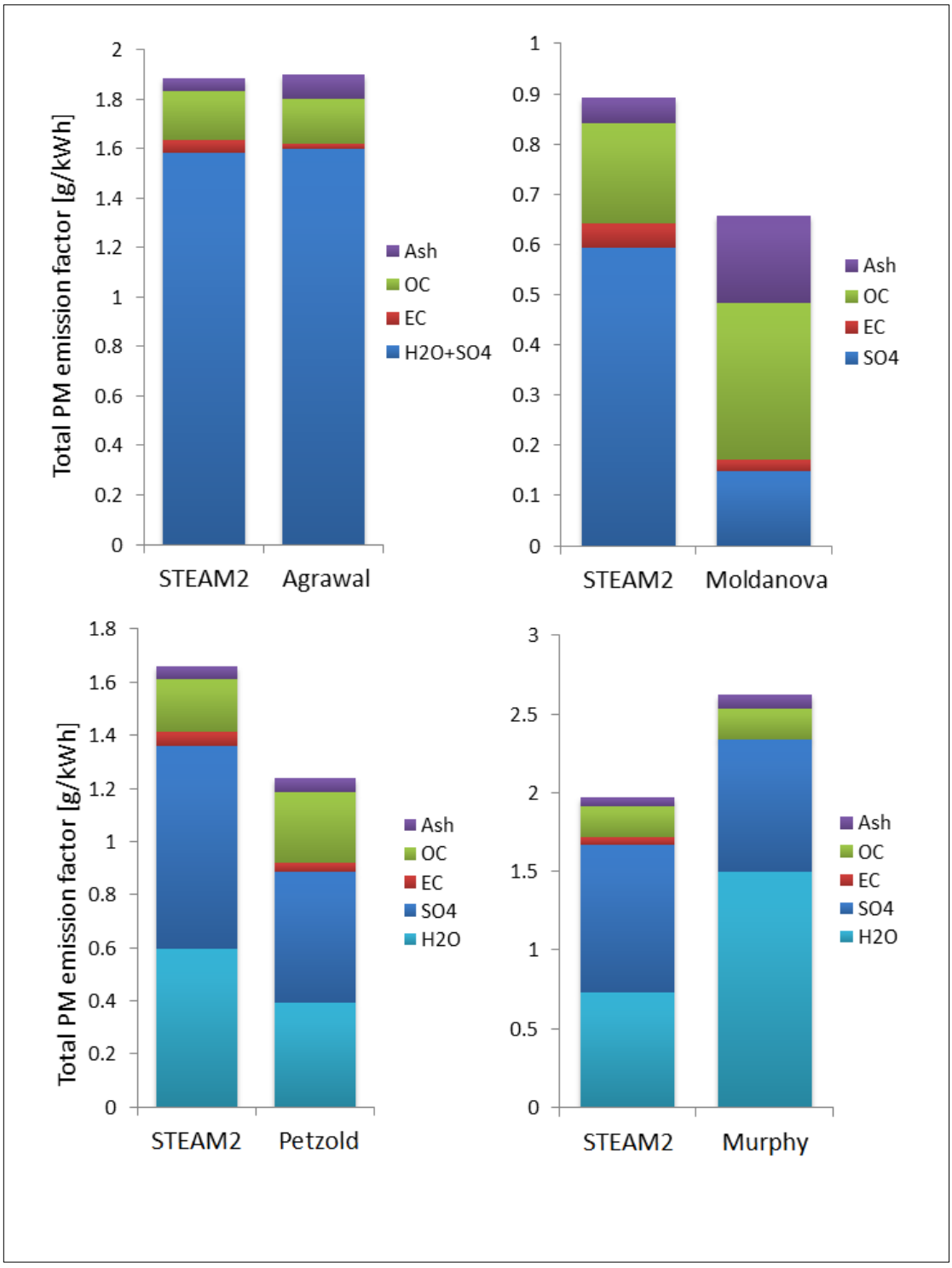

Figure 17a-d: Comparison of the predicted and measured emission factors for the chemical constituents of PM. The measured data has been extracted from Agrawal et al. (2008), Moldanova et al. (2009), Petzold et al. (2008) and Murphy et al. (2009).

The water content of PM in these four datasets varies significantly. This can be due to differences in the experimental setups, sampling conditions and reporting. Water and organic compounds may condense on particulate surfaces after fuel combustion. Dilution and cooling of the PM sample to a lower concentration and temperature have an effect on the amount of condensed water. The amount of water is commonly calculated assuming a constant ratio of SO_4 and water (Agrawal et al., 2010; Agrawal et al., 2008; Petzold et al., 2008). To overcome these difficulties, a dry PM mass could be used instead; however, this would require the inclusion of aerosol condensation processes. In STEAM2, the associated water is modelled separately (according to the IMO GHG2 study), and the user has an option to exclude it.

6. Emission analysis for the Baltic Sea shipping

In this chapter the results produced by the model for marine shipping in the Baltic Sea are presented, which cover the time interval between January 2006 and December 2009. During these years, the maximum sulfur content of marine fuel has been forced to a lower level, economic recession took place and the shipping traffic itself has evolved and shifted. These geographical and quantitative changes in the shipping sector and in their produced emissions are illustrated in this chapter.

There is an ongoing discussion in the International Maritime Organization about the options to curb exhaust emissions of international shipping. These are mostly revolving around the issue of climate change impact and emissions of CO_2, but the principles behind different market based instruments also apply to other pollutants like NO_X, SO_X and PM. According to the study of ENTEC, several options with different benefits and drawbacks are available: First is the "polluting state pays" scenario, which builds on the idea of allocating the emissions of ship traffic according to the flag state of the ship or by geographical area where the actual emissions occur. With these options however, the individual states would still need to find a way to allocate the costs to individual ships eventually, which could be done by imposing taxes using ship specifications such as weight taking travel distances into account. This in turn would require accurate information about how these ship attributes affect the emissions of individual ships.

Another option is an emission trading system (ETS), which relies on emission credits, a system much like to the existing CO_2 credit mechanism already applied in Europe, but in which the shipping sector is not currently included. A more direct option is based on the actual fuel consumption of ships, in which the additional cost is built in to the bunker fuel prices. To illustrate the implications of implementing some these cost allocation methods, the emission shares have been evaluated in this chapter using several of the above mentioned criteria.

6.1 Emissions from Baltic Sea shipping in 2006-2009

The archived AIS data for the years 2006 to 2009 presented in Chapter 4.4 was used to estimate monthly and annual emission estimates for the Baltic Sea. It was observed that the ships encountered in the AIS data can be classified based on their fuel consumption and IMO number. The monthly appearances of these classes are presented in Figure 18.

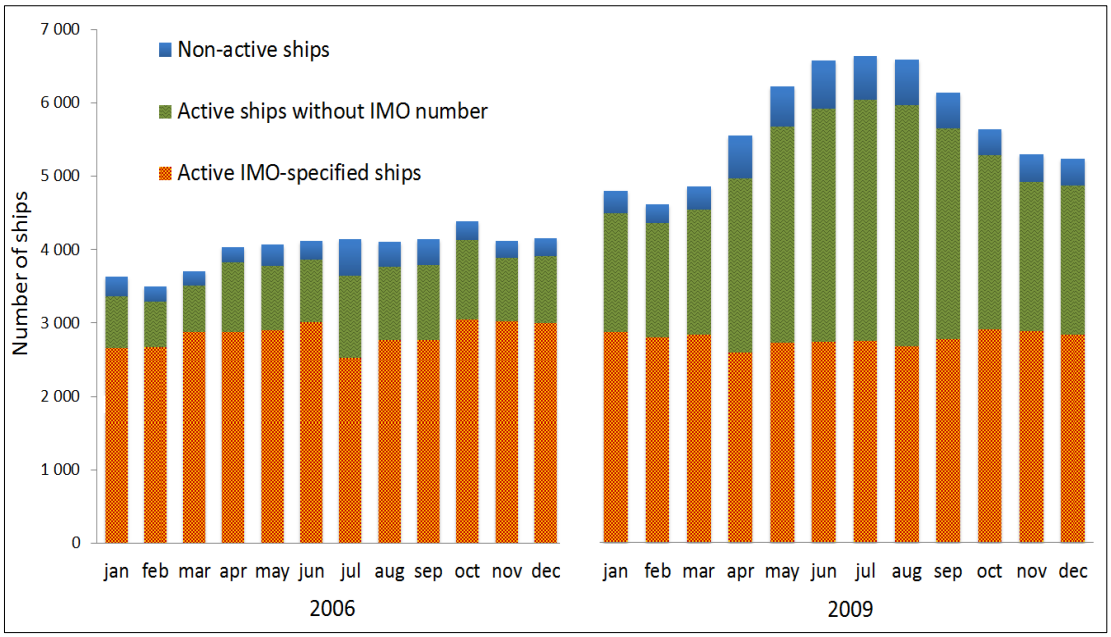

Figure 18: Monthly number of ships according to the archived AIS data in 2006 and 2009. Active ships with IMO number represent the regular and registered marine traffic while ships without the IMO number represent unregistered vessels and are not found in the internal ship database. Non-active ships is the group of vessels appearing in the archived AIS data which do not consume any fuel according to the model or send more than one AIS message in a month.

Ships with an IMO number represent the commercial and regular ship traffic while the rest of the ships are not specified in the internal ship database and are assumed to be small vessels and are thus attributed with generic small tug boat specifications. Besides the data from these active ships, the archived AIS data contains singular messages or a small amount of physically impossible route data from some vessels. Almost all of these "non-active" ships showing in the archived AIS data are of unknown origin but seem to appear more frequently during summer months. In 2009 also the number of active ships without IMO number shows a seasonal dependency which describes the increased passenger and yacht traffic during the summer period in the Baltic Sea area (Figure 18). Moreover, it can also be seen from the figure that while the regular and registered ship amount on the whole remains unaffected by season the total number of vessels are at maximum during summer months due to the increase in non- commercial traffic.

The marine traffic was affected by the economic recession starting from 2008 and continuing throughout 2009. Most of the riparian states showed decreasing gross domestic product (GDP) rates starting from the second quarter of 2008 with a few exceptions: for Denmark the economic difficulties began in the second quarter of 2006

and in Russia after a steady season of growth the inflation adjusted annual GDP growth rate crashed quickly below -9% in the second quarter of 2009 (Trading economics, 2011).

The annual emission estimates according to the model for 2006 – 2009 are listed in Table 5 and monthly time series for NO_X,SO_X, PM and CO emissions covering the whole study period are presented in Figure 19.

Table 5: Emission estimates for 2006 – 2009 in the Baltic Sea. AIS downtime has been taken into account in the figures. Estimates for 2006 are presented in tons and the following years in relation to emissions in 2006. PM emissions are assumed to be equal to the sum of OC, EC, Ash particles and SO_4 with its associated water molecules.

	Pollutant	2006 [tons]	2007 (of 2006)	2008 (of 2006)	2009 (of 2006)
Gases	CO_2	16 490 000	110.50 %	113.90 %	108.90 %
	NO_X	335 900	109.90 %	112.30 %	107.10 %
	SO_X	144 200	91.30 %	91.40 %	86.20 %
	CO	51 640	112.60 %	124.90 %	124.50 %
PM constituents	OC	5 730	109.90 %	112.60 %	107.50 %
	EC	2 220	109.90 %	113.00 %	108.10 %
	Ash	1 620	109.80 %	112.80 %	107.70 %
	SO_4	20 930	91.40 %	91.90 %	86.20 %
PM		30 500	97.20 %	98.50 %	92.90 %

In 2006 a total of $16.5 * 10^9\ kg$ of CO_2 was produced by the marine shipping in the Baltic Sea according to Table 5 while only 5% of the total CO_2 emissions resulted from the ship traffic without certified IMO number. The year 2007 showed a steady increase in overall marine activity resulting in a 10% increase in CO_2 emissions. To put this amount of produced CO_2 into perspective however, the contribution of the traffic in Baltic Sea to the global CO_2 emissions can be estimated to be less than 2 percent according to the second IMO greenhouse gas study in which the total CO_2 emissions were estimated to total $1.046 * 10^{12}\ kg$ in 2007 (Buhaug, 2009).

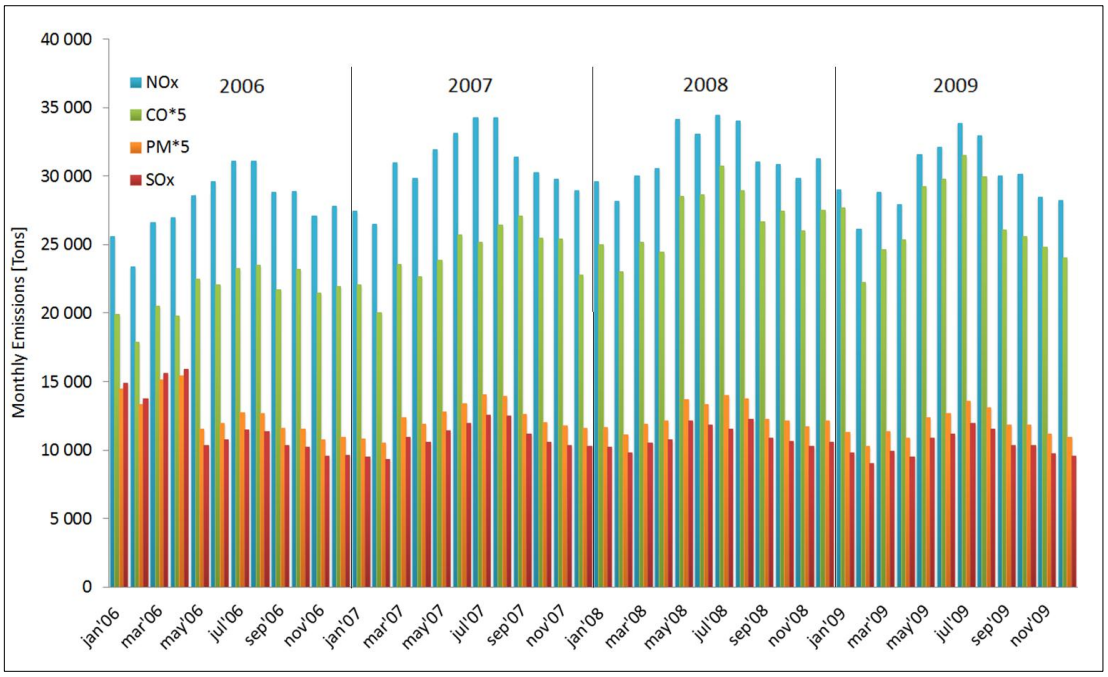

Figure 19: Monthly estimates for NO_X, SO_X, CO and PM emissions during 2006-2009. PM and CO emissions have been multiplied by 5 for enhanced visual clarity.

The overall trend of CO, CO_2 and NO_X emissions was increasing from 2006 to 2008, but decreased during 2009 in relation to the respective emissions in 2008 because of the recession. Regular passenger traffic was least affected by the recession, whereas all of the emissions from containerships and vehicle carriers showed significant decrease signaling a slowdown of business in these sectors. The decrease of all the modeled emissions during 2008 - 2009 was nevertheless no more than 5 % despite the significant decrease of all modelled emissions from Roll-on/Roll-off ships (RoRo), general cargo and containerships; with these particular ship types the modelled emission amounts decreased up to 20% and no less than 14%.

At the end of 2009 a total of $17.8 * 10^9\ kg$ of CO_2 was produced. Due to the increase in the number of unspecified ships during the past years the share of IMO certified ships of the produced CO_2 emissions decreased to 90%. Moreover, the strong simultaneous increase in CO emissions can be explained with the large number of these new unspecified ships; small boats produce relatively large amounts of CO according to the model.

The annual emission amounts of SO_X and SO_4 in respect to the reference year of 2006 have evolved differently than the previously discussed CO, NO_X and CO_2 because of the change in SECA fuel sulphur requirements: in May 19th of 2006 the maximum allowed

sulfur content used in SECA area was decreased from 2.7% to 1.5%. The effect of this reduction is clearly visible in Figure 19. Also a clear seasonal trend in the presented emissions for every year of study can be identified from the figure – for example, in any year of study the (sulfur independent) emissions in July are 16% - 25% larger than in January. The main reason for this is not just the seasonal increase in ship amounts without IMO number (Figure 18) but rather the increase in fuel consumption of the more notable IMO certified ships; e.g. Roll-in/Roll-out passenger ships (RoPax) which are later shown to consume more than one fourth of the total fuel consumption, seem to be significantly more active in the summer time than in winter. Most of the ship types besides RoPax and passenger ships, however, do not show a strong seasonal dependency in their activities.

6.2 Geographical emission changes from 2006 to 2009

Besides the total emission estimates, the STEAM2 model is also capable of presenting the cumulative geographical distribution of the modeled emissions (Jalkanen et al. 2009, 2011). During 2006 – 2009 the annual fuel consumption of marine traffic in the Baltic Sea has increased approximately 9%. At the same time, the reduction of maximum sulfur content of marine fuel has caused reductions in the total SO_X and PM emissions.

To be able to identify where these changes have affected the local air quality the most, a difference map using the aggregate emission data from January - April of 2006 and 2009 was produced (Figure 20a-b).Comparison of the combined monthly emission estimates between January and April in 2006 and 2009 reveals that SO_X emissions in 2009 are 37 % smaller than in 2006. A similar comparison for PM emissions shows a decrease of 26% respectively. However, it can be seen from the figure that the majority of these SO_X reductions reside in the major ship travel routes away from dense human population.

Moreover, as the several areas with positive emission amounts indicate, SO_X emissions in some harbors, most notably in Gdansk and Kiel, have even increased during the study period. One explanation for this result is that the use of auxiliary fuel consumption (consisting of 0.5% sulfur in mass according to model) which is concentrated near harbor areas, is unaffected by the imposed sulfur reducing legislation.

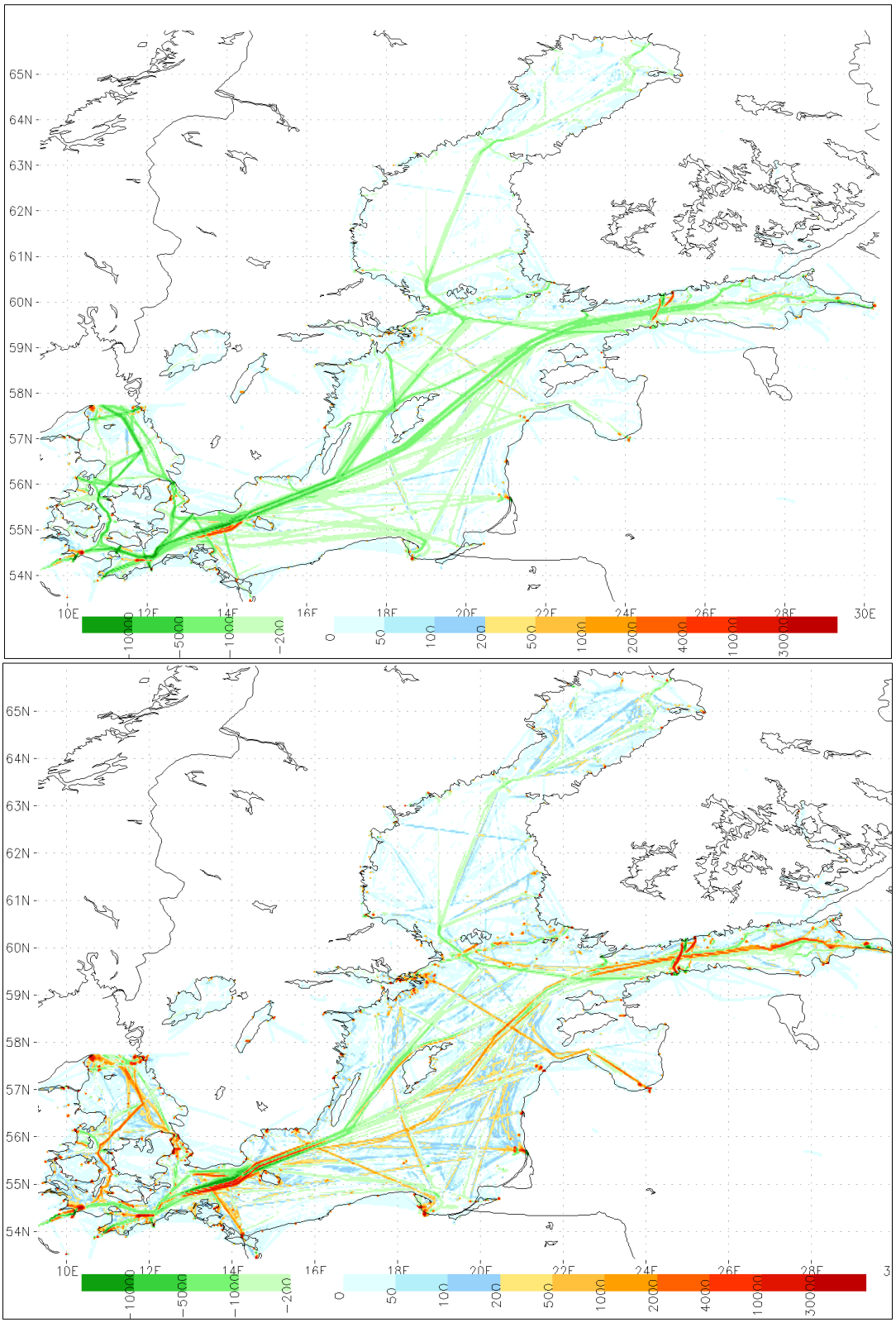

Figure 20a-b: Estimated change in SO_X (a) and NO_X (b) emissions distribution between 2006 and 2009. Total emissions of January - April 2006 have been subtracted from the estimated total emissions of January -April 2009. Green colors indicate the areas where estimated emissions in 2006 surpass the emissions of 2009, while other colors indicate a increase in emissions. The color scale corresponds to emissions in kilograms in an area of 0.03 x 0.03 degrees (approximately 6.5 km^2).

A corresponding difference map was also produced using NO_X emissions (Figure 20b). In addition for evaluating changes in NO_X emission distribution during the study period, it also possible to indirectly identify geographical changes in fuel consumption and travel routes from the figure. The reason for this possibility is that the aggregate NO_X emissions correlate very strongly with aggregate (and even instantaneous) fuel consumption in the model. Unfortunately no emission grid has been produced for CO_2 emissions, which would've been the ideal choice for identifying geographical changes in fuel consumption.

A couple of significant new ship routes (e.g. near Helsinki and Tallinn) can be identified in areas where NO_X emissions in 2009 surpass the estimated emissions in 2006 considerably. Also, many harbors near Denmark, Germany and Stockholm area in 2009 seem to support more marine traffic than in 2006 which might be caused by the increase in small and unidentified ships that most likely operate near the coastline. Furthermore, the marine traffic seems to have been increasing near the Baltic States, St. Petersburg and especially near Helsinki which is partly because of the opening of the new Vuosaari harbor for goods traffic in 2008. The area between Gotland and Oland of Sweden and the whole Gulf of Bothnia are the most notable geographical areas where NO_X emissions and thus presumably the marine traffic has decreased during the study period.

6.2.1 Allocation of emission costs by geographical area

One of the suggested options for emission allocation is based on geographical distribution of emissions, in which the emissions happening inside the economic zone of each country would be included in the national reporting of emissions. Confirming the actual level of emissions with measurement inside each economic zone, however, would be challenging as there are at any given time over 2000 ships sailing the Baltic Sea. Confirming the emission levels through measurements will cost a lot of money and personnel resources and still leaves doubts how to allocate emission to each country. Fortunately, emission distribution estimates by geographical areas such as in Figure 20a-b can be produced with models based on AIS messages such as STEAM2.

6.3 Flag state analysis

The MMSI code contains information about the flag state of the ship thus enabling the comparison of nations in terms of produced emissions of their marine traffic. In Figure

21a, based on the total fuel consumption eleven most contributing flag states for each year in study are presented.

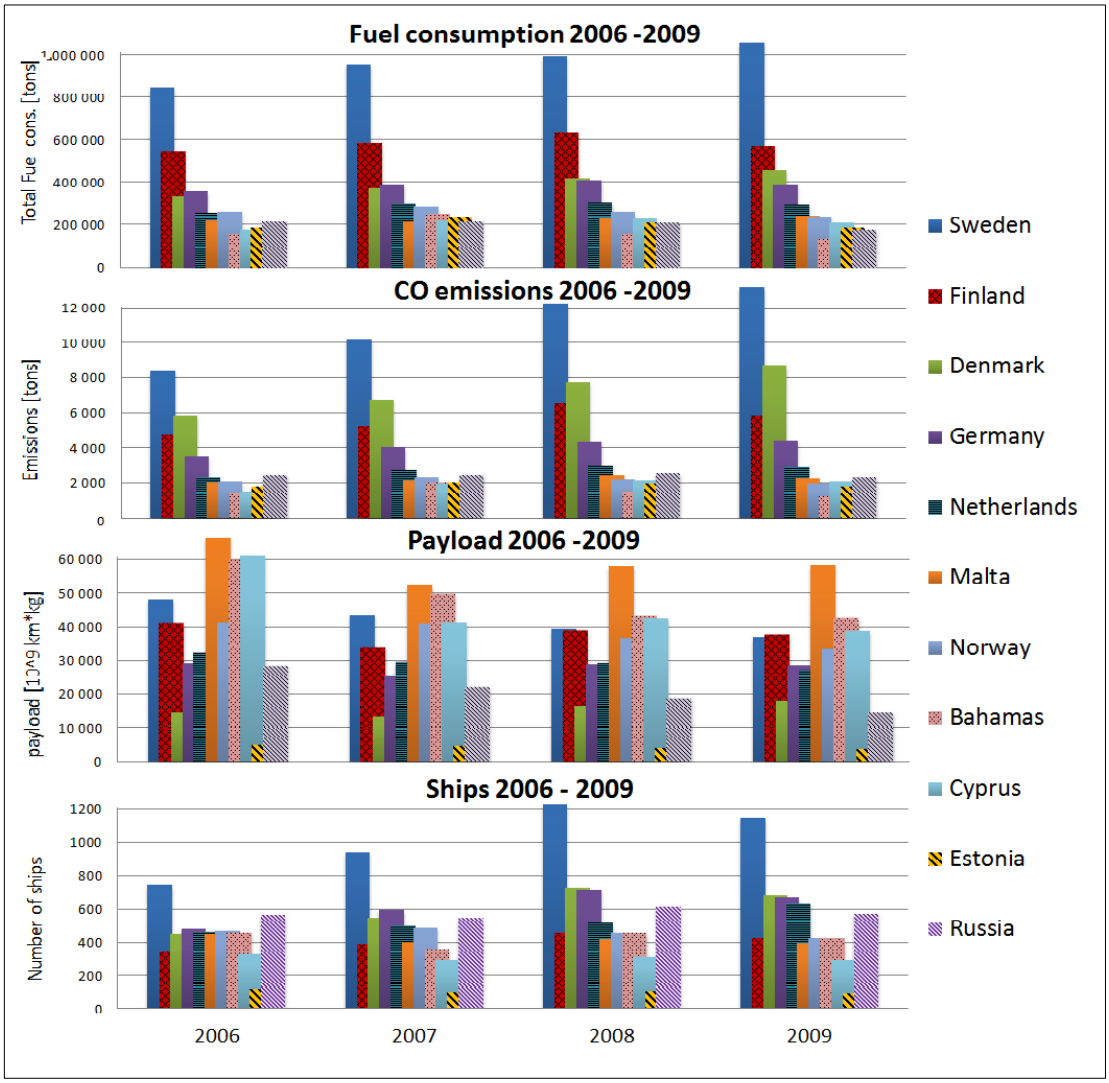

Figure 21a-d: Estimated total fuel consumption (a), CO emissions (b), payload (c) and the fleet size (d) of the eleven most contributing flag states according to flag state information of the MMSI codes. Due to variable AIS data quality and non-optimal travel distance calculation method used in 2006, the respective transferred payload values may have been overestimated up to 20%.

The changes in fuel consumption of the riparian states are similar to their respective changes in GDP with few exceptions: Sweden, which is the undisputed leader in total fuel consumption, is showing steady increase even in 2009 despite the recession. Also Denmark's growth in terms of fuel consumption has been steady and rapid despite its nonexistent GDP development at that time (Trading Economics, 2011). The fleet sailing under the flag of Russia at the Baltic Sea is suspiciously small, resulting to emission estimates that are comparable to those for Estonia. Moreover, the total fuel

consumption of the Russian fleet has decreased during the years in study which coincided with a strong growth period in the Russian economy. Interestingly the ship traffic near Russian harbors presented in Figure 21b is not showing the same decreasing trend.

Aggregate SO_X, PM, and NO_X emissions of fleets tends to correlate strongly with it's aggregate fuel consumption and thus the relations of these emission amounts between the flag states would be similar to those of in Figure 4a and are not presented in this paper. CO emissions however do not share this similarity which can be seen from Figure 21b: If measured in CO emissions, Denmark is the second largest polluter in the Baltic Sea and Denmark's and Sweden's large share of CO indicates that a large portion of the unidentified small vessels are from Denmark and Sweden. Indeed, the Riparian states and especially Sweden, Germany and Denmark account for most of the new ships appearing in the AIS data which can be seen from Figure 21d.

The ships sailing under the flag of Bahamas, Cyprus and Malta are heavy compared to other states: the average gross tonnage (GT) for a Maltan ship is close to 11200 tons and for Bahamas over 14000 tons whereas the average weight for a Swedish ship is less than 2800 tons (in 2009). Furthermore, the abovementioned flag states are also more cargo oriented; From Figure 21c it can be seen that a very large portion of the transferred payload is carried by the fleets of Malta, Bahamas and Cyprus alone. These payload values have been calculated using a ship type specific fraction of deadweight, given by the Technical research center of Finland (VTT, 2011).

The average age of the fleet and its recent development differ among the most contributing flag states significantly. For example, the Russian fleet is the oldest on average in 2009 (25 years) and more than 14 years older than the youngest fleet of Netherlands although the fleet of Finland and Sweden is almost as old as Russia's.

6.3.1 Allocation of emission costs by region or flag state

It is likely that allocating the emissions to the flag state would eventually lead to a situation where the ships in the Baltic Sea will be reflagged to a different country with less strict policies. This would happen even more likely if the flag state emission allocation is done only on regional or European level. The flag state allocation would probably only work if done simultaneously globally in a way that the same rules apply to all flags.

6.4 Emission analysis by ship type and size

According to the model results, the marine traffic in the Baltic Sea is for the most part dominated by eight most contributing ship type classes present in the model's ship database; The top eight accounts for 93% of total emissions in all classes and fuel consumption which applies for all the years in study 2006 - 2009. These ship types and their average attributes in 2009 are presented in Table 6.

Table 6: Most common ship types among the Baltic Sea marine traffic and their average attributes in 2009 according to model shipping statistics. Cargo payload of deadweight tonnage (DWT) is the average fraction of deadweight that is allocable to payload based on calculations by VTT. For containers and RoPax ships, the unit emission is dependent on GT. Unit emission is the estimated amount of CO_2 emissions per transferred payload.

2009	ROPAX	TANKER	GC	CONTAINER	RORO	BULK	PASSENGER
Average GT [ton]	16 560	27 380	4 680	20 770	15 010	25 800	18 440
Average DWT [ton]	3 290	47 140	6 390	24 060	9 030	44 600	2 110
Payload of DWT	0.42	0.5	0.4	0.4-0.65	0.24	0.5-0.6	-
CO_2 unit emission [$g\ km^{-1}kg^{-1}$]	127	8.51	30.6	26.0	67.7	7.32	-
Average age	19.7	8.6	15.8	8.5	15.5	13.9	30.4
Avg. main engine power [kW]	14 700	8 310	2 730	15 660	10 780	7 710	12 440
Avg. service speed [m/s]	9.1	6.7	6.3	9.8	8.8	7.2	7.7
Common engine design	4-stroke	2-Stroke	4-stroke	Both	4-stroke	2-stroke	4-stroke
Total ships in 2009 (change from 2006)	220 (-15)	1 785 (+316)	2 281 (-68)	347 (+106)	152 (-19)	984 (-100)	194 (+33)
Main purpose	Vehicle and passenger travel, cruising	Liquid cargo transfer	General cargo transfer	Container cargo transfer	Vehicle transfer	Bulk cargo transfer	Cruising and passenger travel

RoRo and RoPax ships, besides having several hundred passengers onboard, also transfer cargo on wheels such as trucks and cars whereas passenger ships are more leisure oriented and packed with up to several thousand passengers. Typically the

payload of these vessels is small compared against the cargo ships. RoPax and Passenger ships and ships are the most frequent and regular types which are, on average, traveling in the Baltic Sea on 10 separate months per year. In contrast, unspecified ships without IMO number and bulk carriers travel infrequently and these ships appear only in 3 separate months on average.

During the recent years the order of these ship types by contribution to emissions has been constantly changing with the exception of RoPax, Tankers, and general cargo (GC), which have been the top 3 polluters in the order as presented for every year of study. These emission shares in 2006 and 2009 for each ship type are presented In Figure 22a-b.

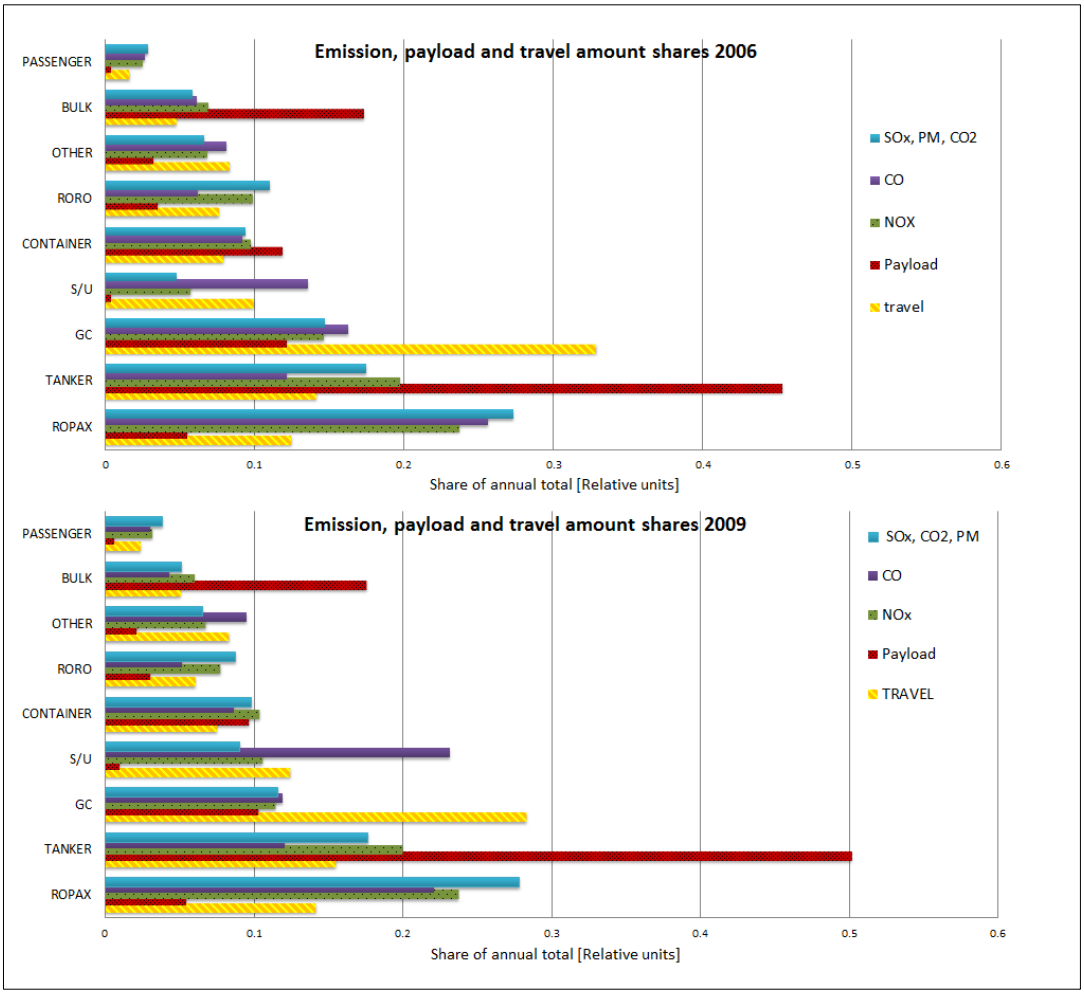

Figure 22a-b: Share of emissions travel and payload in 2006 (a) and 2009 (b) of the most contributing ship types. SO_X, PM and CO_2 emission shares according to model are approximately equal and differs at most ± 1 unit percent from the presented value. S/U refers to small tugs and unspecified ships.

From Figure 22a-b it can be seen that the heavy cargo ship classes are not to be blamed alone to have caused most of the emissions. Indeed, bulk ships which represent the heaviest vessels sailing in the Baltic Sea contribute approximately 5% to total emissions of each modeled type while RoPax ships contribute as much as 25%. Furthermore, the estimated total payload for bulk ships is four times larger than for RoPax ships in 2009. Tankers, which are a mix of several subclasses that include chemical, LNG, liquid petroleum gas (LPG) and other liquid product tankers, are responsible for a half of the total payload transferred across the ocean in 2006 - 2009. Bulk carriers transfer the second biggest amount of payload (approx. 18%), which usually consists of unpackaged cargo such as coal or wood.

Large weight makes a ship sail deeper causing the amount of displaced water and water surface to increase which in turn contributes to the resistance in moving in water. To study the contribution on total emissions of the heaviest ships sailing at the Baltic Sea the estimated emission shares were allocated among different weight classes in 2006 and 2009. The result of this study indicates that ships weighting more than 25000 tons are responsible for approximately 27% of total PM, SO_X, CO_2 emissions in 2006 and in 2009 approximately 33%. Indeed, the role of large ships in the production of emissions has increased throughout the study period. For example in 2006 half of the CO_2 emissions was produced by ships weighting more than 12 250 tons in 2009 by ships weighting more than 14 300 tons respectively. Furthermore, the largest ships (GT > 50000t) are much younger than the smaller ones being only 7 years old in the average which further reinforces the observation of the shift towards larger ships in the Baltic Sea. As it was discussed in Chapter 6.3 it is likely that these heavy vessels are being registered to sail under a surrogate flag such as Malta.

In 2009 the majority of NO_X emissions (61.7%) are being produced by 2971 ships that weight more than 10000 tons. Most of these are bulk carriers and tankers which prefer 2-stroke engines as these ships are heavy and require large power outputs. 2-stroke engines are designed to run with relatively small RPM and because of the longer reaction time for NO_X formation process they also produce significantly more NO_X emissions per produced engine power output. This is the reason why bulk carriers and tankers have relatively large NO_X shares when compared against other emissions classes they have produced.

Interestingly, the usage of main engine fuel and auxiliary fuel is strongly differentiated among the weight classes. For example, in 2009 the largest weight class (GT > 50000 ton) is responsible for using 12.5% of main engine fuel but only 4.9% auxiliary fuel. This relation between the consumption of main and auxiliary fuel is reversed in the smaller weight classes – The contribution of the smallest class is only 5.4% for main fuel but 26.5% for auxiliary fuel. These relations apply qualitatively for every year in study as well.

Even though the weight significantly affects the fuel consumption of any marine vessel, an increase in weight is outweighed by an increase in velocity which is one of the reasons for RoPax ships, with their high average service speed of 9.1 m/s, are having the biggest share of total emissions. On the other hand bulk ships and tankers travel with speeds lower than 14 and with this combination of relative low service speed and large cargo capacity they are the most economical classes having by far the smallest unit emission per transferred payload (Table 6).

6.4.1 Allocation of emission costs by individual fuel consumption

The option of introducing an additional environmental tax to the ship fuel prices is probably the simplest way of allocating the environmental tax burden in the ship. This option however poses a problem as it leaves several important administrative questions open, like who will administer the emission fund which is collected as a part of the fuel price.

If this method for cost allocation would be implemented, it is apparent that RoPax ships would suffer the most and might even force some significant RoPax/RoRo dependent enterprises out of business because of the inevitable increase in fuel prices. Also, some of the current cargo flow over the Baltic Sea might transported by alternative methods (e.g. by road or by train) in the future – A scenario which should be studied thoroughly.

7. Conclusions

In this thesis, an extended and improved model version of the original marine shipping model (Jalkanen et al., 2009) was introduced. It's capability to evaluate power requirements and fuel consumption was validated and the model was used to produce various emission estimations and shipping statistics for the past few years. Also, further improvements for the model were presented and difficulties arising from using AIS data for emission estimation the model were discussed.

7.1 Conclusions from the emission estimation model

The use of the AIS data facilitates an accurate mapping of the ship traffic, including the detailed instantaneous location and speed and of each vessel in the considered area. The presented model allows for the influences of a comprehensive range of relevant factors, including accurate travel routes and ship speed, engine load, fuel sulphur content, multiengine setups, abatement methods and waves. The presented model is the only method in the available literature that includes such a range of effects.

In previous emission inventories of marine traffic, constant emission factors have commonly been used. However, in order to obtain accurate predictions, at least the dependence of shipping emissions on engine load has to be taken into account. This is especially important in port areas, as the European sulfur directive (EC/2005/33) states that the fuel used in EU harbor areas must not contain more than 0.1 % sulfur since the beginning of 2010. This directive will have a significant impact on the PM emissions from ships at berth, which should be taken into account by any model used in local scale modeling of harbor regions. It is important to be able to reliably evaluate the effects of the policy options that focus on reducing the PM emissions from ships. The health and climatic influences can be substantially different for the various chemical constituents of PM; the modeling should therefore disaggregate the PM emissions from ships accordingly.

The relatively largest uncertainties of the model predictions presented probably arise from the use of various types of fuel (Hulskotte and Denier van der Gon, 2010). It is challenging to extract the detailed data regarding the fuel types used in ships in various geographical areas. However, if the data is available on the fuel type or the sulphur content, the model can adjust itself accordingly, and provide emissions, facilitating also various abatement strategies. Another challenge is the scarcity of detailed composition-

resolved experimental data on PM emissions. The emissions of the chemical components of PM should be analyzed at various engine loads, and using various fuels, in order to be able to more comprehensively analyze and evaluate the performance of the modeling approaches. Finally, in the future the model should be properly validated against direct emission measurements and not just instantaneous power measurements. However, some direct emissions measurements taken above a marine vessel have already been analyzed and the model's prediction accuracy compared to these data looks promising.

7.2 Conclusions from the emission estimates for 2006 - 2009

The estimated emissions of the reference year of 2006 were presented in Chapter 6.1. In 2007, based on fuel consumption and most of the modeled emission classes, Baltic marine traffic increased approximately 9% in respect to 2006. The late economic recession is clearly visible in the emission estimates – The increasing trend of Baltic Sea shipping significantly slowed down in 2008, which resulted in just 3% more emissions than in 2007. The recession began to affect marine traffic the hardest in 2009 diminishing total fuel consumption and emissions to a level, which was a couple of percent lower than in 2007.

Maximum allowed fuel sulphur content was decreased in May 2006 from 2.7% to 1.5% and the effect of this reduction was studied. Total SO_x emissions in 2006 and 2009 between January to April was compared, and even though fuel consumption was 9% larger during the interval of 2009, SO_X emissions were calculated to be approximately 37 % smaller in that time. A similar comparison revealed that PM emissions had dropped 26% respectively. However, the majority of these reductions reside in the major ship travel routes away from dense human population. It would be worthwhile to investigate if this reduction in sulfur dependent emissions has had a significant effect on the health of the coastal population, and also, what has been the indirect cost of this directive.

Furthermore, in the forthcoming years the sulfur content of the marine fuel is to be further reduced, possibly to a final level of 0.1% in the SECA area. It has been estimated that the resulting increase in fuel prices after such a reduction will induce costs of several billion euros for the Baltic shipping. In Chapter 6 it was discussed that there are several methods how the costs of this directive can be allocated - With quite

different outcomes. Therefore, it would be very important to estimate the health benefits and costs of the possible changes due to the directive thoroughly.

Analysis by flag state showed a steady increase in terms of fuel consumption from Sweden despite the recession, in contrast to Finland and Germany. Denmark is closing in on Finland in produced CO_2 emissions. Indeed, Denmark's growth has been rapid and if this trend continues unchanged, Denmark should surpass Finland in the forthcoming years in all produced emission classes. In contrast, the fleet sailing under the flag of Russia is surprisingly small which results to emission estimates that are comparable to those for Estonia. Moreover, the Russian ship traffic has been steadily decreasing according to AIS data while the geographical emission distribution near Russian harbors does not support this downshift in Russian marine activity in the Baltic Sea.

The ships sailing under the flag of Bahamas, Cyprus and Malta are very heavy and cargo oriented. Therefore, their share of transferred payload is significant. It is to be suspected that increasingly more heavy vessels are switching the flag state to those mentioned above to be able to use cheaper fuel in the expense of emissions. It might prove worthwhile to investigate the amount of Russian marine traffic that sails under a proxy flag state and also, the motivation behind this phenomenon – if emissions are to be reduced by setting stringent legislations then those legislations should not be avoided by changing the flag state.

Eight most contributing ship type classes account for 93% of total emission and fuel consumption. RoPax-ships are the undisputed number one in this measurement, followed by tankers and general cargo ships. The recession affected container ships, general cargo and RoRo the most. Surprisingly, RoPax ships contribute approximately 17% to total transferred tonnage over the sea surface, but manages to contribute to total emissions more than 27%. In contrast, with energy efficient tankers and bulk cargo ships, this relationship between transferred tonnage and emissions is reversed. One explanation for this is that RoPax ships sail with relatively high speeds and thus the resistance from water is significantly greater for RoPax ships.

The average main engine power and weight is slightly on the increase (tankers + 10%) while the total travel distance is decreasing. This trend indicates that ship owners prefer bigger ships and shorter travel amounts.

2-stroke engines dominate the largest weight classes starting from 10000t and up and ships in these weight classes are responsible for the majority of NO_X emissions (61.7%). Therefore, an effective way to reduce NO_X emissions would be to reduce emissions from these ships.

7.3 Further improvements

The extended model presented in this thesis can be further improved in several ways. Most importantly, with slight modifications it can be used for other marine regions besides the Baltic Sea, if proper input data for the model will be available. However, the AIS data cannot be received across extensive sea areas, unless a satellite-based AIS reception is used. International cooperation between maritime authorities is therefore needed to be able to extend the model into a global scale. In case the model is extended for other marine regions still counting on the VHF-based AIS messaging, the implementation if more intelligent interpolation feature is needed.

The power estimation process is arguably the most important part in the model and it has been totally renewed since the previous version; without accurate power estimates, even the engine load modeling loses its purpose. Fortunately, the detailed Hollenbach method's prediction accuracy was shown to be great. If the initial information about the ship's spatial attributes are not precise however, then the Hollenbach method should not be able to produce better results than a much more simple estimation process would. Because of this, rather than making efforts to enhance the method for power estimation, it might prove fruitful to model some of the more important factors that are currently not accounted for, for example, the effect of ice and sea currents. It has been calculated that adding sea currents would affect the power estimate even more than the effect of waves which has been included in the model in an early phase. Furthermore, implementing sea currents should be relatively straightforward although tides and seasonal changes might cause difficulties at open sea areas.

The most important area for geographical emission estimates are the most densely populated harbor areas. To be able to accurately account for the emissions near harbor area then acceleration and kinetic energy of the ship can be taken into account. This implementation requires the speed data to be smoothed, which in turn might reduce the undesired variance in power estimates which are caused by even the slightest speed changes while the ship is travelling near its service speed. Moreover, a proper use of

acceleration data allows the monitoring of changes in engine load and thus CO emissions spikes can be accurately modeled and might even enable the assessment of unidentified ship's attributes.

The chemistry involving emissions in a diesel combustion process is complex to say the least. Furthermore, engines vary significantly in size, speed and power and thus general rules about emission factors are difficult to establish. Still, the SFOC concept as general driver for emissions is intuitive and the results are backed by other studies in literature. However, the logic behind the effect of fuel consumption to emissions is currently in slight contradiction as was presented in Chapter 4.5 and the logic behind it should be generalized if possible. To achieve this, more measurement data for PM emissions against instantaneous fuel consumption is needed, especially for 4-stroke engines. At the same time, NO_X emission measurements from a 4-stroke engine might lead to a more sophisticated NO_X emission modeling process based on combustion time.

References

[1] Agrawal H., et al. 2010. Emissions from main propulsion engine on container ship at sea. Geophys. Res., 115 (2010) D23205.

[2] Agrawal, H., et al. 2008. Emission measurements from a crude oil tanker at sea. Environ. Sci. Tech., 42 (2008) 7098.

[3] Andreae, M. O., Gelencsér, A. 2006. Black carbon or brown carbon? The nature of light-absorbing carbonaceous aerosols. Atmos. Chem. Phys. 6:3131-3148

[4] Buhaug, Ø., et al. 2009. Second IMO GHG study. International Maritime Organization (IMO) London, UK.

[6] Cooper, D. A. 2003. Exhaust emissions from ships at berth. Atm. Env. 37 3817.

[7] Cooper, DA. 2001. Exhaust emissions from high-speed passenger ferries. Atm. Env., 35 (2001) 4189.

[8] Corbett, J.J., et al. 2007. Mortality from ship emissions: a global Assessment. Env. Sci. Tech., 41 (2007) 8512.

[9] Corbett, J.J., et al. 2010. Arctic shipping emissions inventories and future scenarios, Atmos. Chem. Phys., 10 (2010) 9689.

[10] De Meyer, P., Maes, F., Volckaert, A. 2008. Emissions from international shipping in the Belgian part of the North Sea and the Belgian seaports, Atm. Env., 42 (2008) 196.

[11] DNV. 2011. Greener shipping in North America.
http://www.dnv.com/resources/reports/greener_shipping_north_america.asp.
Visited 10.4.2011

[12] European Environment Agency. 2009. Air pollutant emission inventory guidebook 2009, Technical guidance to prepare national emission inventories, EEA Copenhagen.

[13] Eyring, V., et al. 2010. Transport impacts on atmosphere and climate: shipping. Atm. Env., 44 (2010) 4735.

[14] Fridell, E, Steen, E, Peterson, K. 2008. Primary particles in ship emissions, Atm. Env., 42 (2008) 1160.

[15] Harati-Mokhtari, A., et al. 2007. Automatic Identification System (AIS): Data reliability and human error implications. The journal of navigation. 60. 373-389. The Royal institute of navigation.

[16] Hollenbach, K.U. 1998. Estimating resistance and propulsion for single-screw and twin screw ships, Ship Technology Research, 45/2.

[17] Holtrop, J, Mennen G.G. 1982. An approximate power prediction method. International Shipbuilding Progress, p.166 and 253.

[18] Hulskotte, J.H.J., Denier van der Gon, H. 2010. Fuel consumption and associated emissions from seagoing ships at berth derived from an on-board survey. Atm. Env., 44 (2010) 1229.

[19] Hänninen, O., et al. 2011. European Perspectives on Environmental Burden of Disease - Estimates for Nine Stressors in Six European Countries. National Institute for Health and Welfare (THL)

[20] International Maritime Organization (IMO). 1998. Regulations for the prevention of air pollution from ships and NOx technical code, Annex VI of the MARPOL convention 73/78, London

[21] Jalkanen, J.-P., et al. 2009. Modelling system for the exhaust emissions of marine traffic and its application in the Baltic Sea area. Atmos. Chem. Phys., 9 (2009) 9209.

[22] Johansson, L. O. 2011. Reactive vehicle routing using a shortest path network algorithm. Aalto University. Laboratory of systems analysis. Espoo

[23] Kasper, A., et al. 2007. Particulate emissions from a low-speed marine diesel engine, Aerosol Sci. Tech., 41 (2007) 24.

[24] Lack, D. A., et al. 2009. Particulate emissions from commercial shipping: Chemical, physical, and optical properties. Geophys. Res., 114 (2009) D00F04.

[25] Matthias, V., et al. 2010. The Contribution of Ship Emissions to Air Pollution in the North Sea Regions, Env. Poll., 158 (2010) 2241.

[26] Matulja, D, Dejhalla, R. 2007. A comparison of a ship hull resistance determined by different methods, Eng. Rev., 27-2 (2007) 13-24

[27] Moldanová, J., et al. 2009. Characterization of particulate matter and gaseous emissions from a large ship diesel engine, Atm. Env., 43 (2009) 2632.

[28] Murphy, S.M., et al. 2009. Comprehensive simultaneous shipboard and airborne characterization of exhaust from a modern container ship at sea, Environ. Sci. Tech., 43 (2009) 4626

[29] Paxian A., et al. 2010. Present-Day and Future Global Bottom-Up Ship Emission Inventories Including Polar Routes, Environ. Sci. Tech., 44 (2010) 1333.

[30] Petzold, A., et al. 2008. Experimental studies on particle matter emissions from cruising ship, their characteristic properties, transformation and atmospheric lifetime in the marine boundary layer, Atmos. Chem. Phys., 8 (2008) 2387.

[31] Petzold, A., et al. 2010. Physical properties, chemical composition and cloud forming potential of particulate emissions from a marine diesel engine at various load conditions, Env. Sci. Tech., 44 (2010) 3800-3805.

[32] Sarvi, A., Fogelholm, C.-J., Zevenhoven, R. 2008. Emissions from large-scale medium-speed diesel engines: 1. Influence of engine operation mode and turbocharger, Fuel Proc. Tech., 89 (2008) 510.

[33] Sarvi, A., Fogelholm, C.-J., Zevenhoven, R. 2008. Emissions from large-scale medium-speed diesel engines: 2. Influence of fuel type and operating mode, Fuel Proc. Tech., 89 (2008) 520.

[34] Schrooten, L., et al. 2009. Emissions of maritime transport: A European reference system, Sci. Tot. Env., 408 (2009) 318.

[35] Schreier, M. et al. 2006. Impact of ship emissions on microphysical, optical and radiative properties of marine stratus: A case study. Atmos. Chem. Phys., 6, 4925–4942.

[36] Townsin, R.L. 1979. The Naval Architect, RINA

[37] Trading economics. 2011. http://www.tradingeconomics.com. USA, New York City. Visited 21.7.2011

[38] VTT. Unit emissions of vehicles in Finland. http://www.lipasto.vtt.fi/yksikkopaastot/tavaraliikennee/vesiliikennee/tavara_vesie.htm. Visited in 10.7.2011

[39] Wärtsilä 46th Project guide. 2007. http://www.wartsila.com/en/engines/medium-speed-engines/Wartsila46. Visited in 1.2.2011

[40] Watson, D. 1998. Practical Ship Design, Elsevier, Oxford, UK, pp 219.

[41] Watson, D. et al. 1976. Some ship design methods. Royal Institute of Naval Architects. RINA

[42] Wild Y. 2009. Refrigerated containers and CA technology. Container Handbook, Vol 3, Gesamtverband der Deutschen Versicherungswirtschaft e.V., Berlin.

[43] Winnes, H., Fridell E. 2010. Particle emissions from ships: Dependence on fuel type, Journal of Air & Waste Management Association, 59 (2010) 1391.

[44] Winnes, H., Fridell, E. 2010. Emissions of NOx and particles from Maneuvering Ships. Transportation Research D, 15 (2010) 204.

[45] Prockop LD, Chichkova RI. 2007. Carbon monoxide intoxication: an updated review. Journal of the Neurological Sciences 262 (1-2): 122–130)

[46] Zbaraza, D. 2004. Natural gas use for on-sea transport. University of Science and Technology, Cracow, Poland.

[47] Brunekreef, B., Holgate, S. 2002. Air pollution and Health. THE LANCET .Vol 360 October 19, 2002

[48] Starcrest Consulting Group. 2008. Port of Los Angeles - Inventory of Air Emissions 2007. Poulsbo, WA